

**Assessing changes and predictability of crop yields and failure risk in the United States:
The Impact from Large-scale Climate Circulations**

by

Taylor A. Schillerberg

A thesis submitted to the Graduate Faculty of
Auburn University
in partial fulfillment of the
requirements for the Degree of
Master of Science

Auburn, Alabama
August 3, 2019

Keywords: Climate variability, crop yield, climate oscillations, teleconnections

Approved by

Di Tian, Chair, Assistant Professor of Crop, Soil and Environmental Sciences
Senthold Asseng, Professor of Agricultural and Biological Engineering, University of Florida
Ruiqing Miao, Assistant Professor of Agricultural Economics and Rural Sociology
Brenda V. Ortiz, Associate Professor of Crop, Soil and Environmental Sciences

Abstract

The weather of the growing season influences crop production and yield. These changes in crop yields can result in economic loss and increases in global food insecurity drastically especially when high production areas are threatened. Seasonal influences on crop yields may be in part due to climate oscillations, which have been linked to floods and droughts. This study will focus on analyzing the impact of climate oscillations on summer (maize) and winter (winter wheat) crop yields from 1960 to 2016 in the rainfed United States, a region affected by several climate oscillations, including Atlantic Multidecadal Oscillation (AMO), North Atlantic Oscillation (NAO), El-Niño Southern Oscillation (ENSO), Pacific Decadal Oscillation (PDO), and Pacific-North American (PNA).

The first chapter of this thesis is to explore and assess the linkage of crop yields variability and climate oscillations. Principal Component Analysis (PCA) shows the first five rotated principal components explain over 70% of the spatial and temporal variability of crop anomalies. AMO is strongly associated with the first rotated principal component. Linear regressions support previous findings that the reproductive period is the most sensitive period for yield forecasting. Categorical yields (low yields below the 30th percentile and high yields above the 70th percentile) are well predicted by climate oscillations using Random Forest, with AMO as the leading predictor in nearly half of maize and a third of winter wheat climate divisions.

The second chapter assesses changes of crop failure, defined as the lower quartile of yield anomalies, influenced by climate oscillations. A Bayesian approach is used to assess crop failure

risk. The results show that positive AMO and negative PNA phases greatly increase maize crop failure. For winter wheat positive NAO increases frequencies of crop failure. Combinations of climate oscillation phases show a positive AMO and negative PDO increase maize crop failure for the majority of the study area, while a negative AMO and any phases of PDO combination increases winter wheat crop failure. The second combination, ENSO and PDO, show that when the oscillations are out-of-phase, the largest changes to crop failure frequencies are experienced.

The findings from this work have implications for improving seasonal forecasting of yields, risk management, and seasonal decision making for various stakeholders. To expand on these findings, future work in this area can include different crops and include other sources of data. By including other data sources, event case studies can be conducted to validate crop loss causes. Combinations of climate indices can be analyzed in more detail. These additional measures would further contribute to the understanding and improvement of seasonal forecasting in the rainfed United States.

Acknowledgments

First, I would like to express my sincere appreciation to my advisor, Dr. Di Tian, for the guidance and support throughout this master degree project. Thanks are also extended to the members of my committee: Dr. Senthold Asseng, Dr. Ruiqing Miao, and Dr. Brenda Ortiz for their valuable suggestions.

Second, I would like to thank my family for their never ending support and love. My father and mother, Daron and Deb Schillerberg, and sister Jess Schillerberg thank you for coming down in my greatest time of need. To my aunt, Karen Nelson and cousin Abby Reese, thank you for visiting me.

Finally, my friends near and far. Especially, thank you to the Auburn friends that welcomed me into their arms, supporting me through the highs and lows. To my friends afar thank you for keeping in touch reminding me of the snowy and wet weather in Iowa.

Table of Contents

Abstract	ii
Acknowledgments	iv
List of Tables	viii
List of Figures	ix
List of Abbreviations	xii
Literature Review.....	1
Climate Oscillations	2
Climate Oscillations and their impacts on crops	5
Maize and Winter Wheat	7
Objectives	8
Chapter 1 Spatiotemporal patterns of maize and winter wheat yields in the United States: predictability and impact from climate oscillations.....	10
Abstract	10
1. Introduction	12
2. Data and Methods	16
<i>2.1 Study Region</i>	16

2.2 Crop yield data	16
2.3 Climate data.....	17
2.4 Data analysis	19
3. Results and Discussion.....	22
3.1 Patterns of spatial-temporal variability of crop yields	22
3.2 Correlations between principal components of crop yields and climate indices	24
3.3 Responses of crop yields to changes in phases of climate indices	28
3.4 Discussing Plausible causations of crop yield patterns due to climate oscillations.....	29
3.5 Predicting crop yield anomalies and categories using climate indices	32
4. Conclusions.....	34
Chapter 2 Crop failure risks changes in the United States associated with large-scale climate oscillations	50
Abstract.....	50
1. Introduction.....	51
2. Data and Methods	54
2.1 Study Area	54
2.2 Yield data and climate indices	55
2.3 Bayesian Analysis	56
3. Results and Discussion.....	58
3.1 Time series of crop failure	58
3.2 The impact of individual climate oscillation on maize crop failure frequencies	59

3.3 <i>The impact of individual climate oscillation on winter wheat crop failure frequencies</i>	61
3.4 <i>The combinations of climate oscillations impact on crop failure frequencies</i>	64
4. Conclusions	66
Recommendations for future research	76
References	77

List of Tables

Table 1.1 The explained variance of the five rotated principle components.	36
Table 1.2 Random Forest variable ranking for maize and winter wheat. Rank 1 signifies the most important variable to determine yield. Values are determined by the number of climate index occurrences for each ranking for all climate divisions.	37
Table 2. 1 The number of climate divisions that experience a significant increase in crop failure at the 90th percentile for maize and winter wheat under different phases of climate indices.	69
Table 2.2 The number of climate divisions that experience a significant increase in crop failure at the 90th percentile for maize and winter wheat under different combinations of AMO and PDO phases.	70
Table 2.3 The number of climate divisions that experience a significant increase in crop failure at the 90 th percentile for maize and winter wheat, while experiencing the indicated combination climate oscillation phases of ENSO and PDO.	71

List of Figures

- Figure 1.1 The study region is highlighted in green. Climate divisions in the study region are contoured in black, counties in gray. 38
- Figure 1.2. The number of climate divisions that have the specified years of data. The original data (blue line) was filled, if under the threshold, first using moving mean (red line) with a 10 year window. Second with KNN Imputation (yellow line), nearest neighbor. A five year moving average was applied and detrended. The number of climate divisions remaining for the maize data is 240 while winter wheat has 222. 39
- Figure 1.3 Patterns of spatial and temporal variability for maize yields, as revealed by the rotated principal component analysis (PCA). Spatial plot A is the loadings for the first principal component (PC1), B is for PC 2, C is for PC 3, D is for PC 4, and E is for PC 5. 40
- Figure 1.4 Same as in Figure 1.3, but for winter wheat. 41
- Figure 1.5 Correlation matrix of rotated principal components and the climate indices during the vegetative and reproductive growing periods for maize (Left Panel). Correlation matrix of rotated principal components and the climate indices during the dormant and reproductive growing periods for winter wheat (Right Panel). * Denotes significant values identified by t-test. Circled are significant values at the 95% level identified using a Monte Carlo approach. 42
- Figure 1.6 PC scores for maize (column 1) and winter wheat (column 2). Significant Monte Carlo (solid and dashed) and t-test (dash-dotted and dotted) results are plotted. Climate

indices were significant for the Monte Carlo test were also significant for the t-test. PC scores are indicated by the thick black line, negative correlations have been multiplied by -1 for easier comparison..... 43

Figure 1.7 Correlation values between yield and climate indices. Dark blue values indicate stronger negative correlations and dark red values indicate climate division with strong positive correlations. 44

Figure 1.8 The differences between average yields during upper tercile and lower tercile of each climate index. A t-test was utilized to determine the significance at the 95% level, represented by the hatched regions. (A) AMO, (B) NAO, (C) PDO, (D) PNA, and (E) ENSO. A larger difference in yield anomalies is indicated by darker colors. 45

Figure 1.9 The correlations between climate indices and surface climate variables during the reproductive period of maize. 46

Figure 1.10 The correlations between climate indices and surface climate variables during the reproductive phase of winter wheat. 47

Figure 1.11 Adjusted R^2 of linear regression for (A) Vegetative and (B) Reproductive phase for maize and the (C) dormant and (D) reproductive phase for winter wheat..... 48

Figure 1.12 The spatial representation of the Brier Score for maize and winter wheat; high yields (A and D), average yields (B and E), and low yields (C and F). A Brier score value of 0 indicates a perfect forecast..... 49

Figure 2.1 Time series displaying the percent of climate divisions experiencing crop failure for maize and winter wheat in the eastern United States..... 72

Figure 2.2 Annual crop failure frequency of maize (left) and winter wheat (right) during each phase of climate indices. Climate divisions with blue coloring indicate a decrease in crop

failure relative to the posterior distribution, while red divisions indicate an increase.

Hashed climate divisions indicate significant increase in crop failure frequency at the 90th percentile..... 73

Figure 2.3 Annual crop failure frequency of maize during phase combinations of AMO and PDO for maize (four left images) and winter wheat (right four images). Climate divisions with blue coloring indicate a decrease in crop failure relative to the posterior distribution, while red divisions indicate an increase. Hashed climate divisions indicate significant increase in crop failure frequency at the 90th percentile. 74

Figure 2.4 Same as in Figure 3 but for ENSO and PDO phase combinations..... 75

List of Abbreviations

AMO	Atlantic Multidecadal Oscillation
EA	Easter Atlantic
EAWR	Eastern Atlantic Western Russia
ENSO	El- Niño Southern Oscillation
EOF	Empirical Orthogonal Function
KNN	K-Nearest Neighbors
LAI	Leaf Area Index
MJO	Madden-Julian Oscillation
NAO	North Atlantic Oscillation
NASS	National Agricultural Statistic Service
NCDC	National Climatic Data Center
PC	Principal Component
PCA	Principal Component Analysis
PDO	Pacific Decadal Oscillation
PDSI	Palmer Drought Severity Index
PNA	Pacific North American
R ²	Coefficient of determination
SCAND	Scandinavian
SST	Sea Surface Temperature

T_{\max} Maximum temperature
 T_{\min} Minimum temperature
USDA United States Department of Agriculture

Literature Review

In the modern era, the world has become more interconnected through trade and technology advances. Nearly 40% of the total global land area is devoted to agricultural purposes such as grazing and cropland. Of the global land, only a quarter produces nearly three-quarters of the global cereal (i.e., maize, wheat, barley, etc.) crop (Foley et al., 2005; Janetos et al., 2017). These regions are usually technologically advanced countries such as the United States, China, and Europe, where crops such as maize and wheat cover the majority of cropland. Little crop diversity can create enhanced vulnerability if disasters such as pest or drought occur, which may reduce crop yields decreasing exports. These and other environmental, political, and economic factors can cause decreases in yields in countries that rely on imports and aid from major crop producing regions (Akresh, Verwimp, & Bundervoet, 2011; Oerke, 2006). Food prices increase as exports are reduced, causing increases in food insecurity, especially in eastern and southern Africa, Latin America, and other regions (Gbegbelegbe, Chung, Shiferaw, Msangi, & Tesfaye, 2014).

Crop yield variability is primarily due to pests, disease, political turmoil, and environmental factors like climate variability. For example pests and diseases are able to be spread among fields through shared farm equipment, widespread heat and drought can cause severe reductions in yield and crop failure, and flooding can cause delay in planting or prevent producers from getting into fields reducing yields (Baum, Archontoulis, & Licht, 2019; Chahal, Aulakh, Jugulam, & Jhala, 2015; Gaupp, Pflug, Hochrainer-Stigler, Hall, & Dadson, 2017;

Goodwin, 2001; Lesk, Rowhani, & Ramankutty, 2016; Teixeira, Fischer, van Velthuisen, Walter, & Ewert, 2013). One-third of crop yield variability can be attributed to climate variability (Ray, Gerber, Macdonald, & West, 2015). Climate variability of the growing season influences crops through anomalies in temperatures and precipitation regimes. The climate variability due to large scale atmospheric-ocean circulation influences global patterns of temperature and precipitation through teleconnections. Teleconnections are the connection of meteorological phenomena of global locations through atmospheric-ocean circulations (Wallace & Gutzler, 1981).

There are several global atmospheric-ocean circulations, also known as climate oscillations because of their cyclic nature. Common oscillations are the El Niño Southern Oscillation (ENSO) and the Madden-Julian Oscillation (MJO). The MJO will not be discussed in this paper, as its effects are primarily felt in the western United States (Zhang, 2005). These climate oscillations among others affect two-thirds of global cropland and have impacts on hurricane frequency, the onset of spring, health, and other socio-economic factors (Heino et al., 2018; Kovats, Bouma, Hajat, Worrall, & Haines, 2003; Trenberth & Shea, 2006).

Climate Oscillations

ENSO is perhaps one of the most researched climate oscillations, and one of the three oscillations originating from the Pacific Ocean. ENSO is measured from SST anomalies in the tropical Pacific Ocean, having an oscillation period of 2-7 years (Cole & Cook, 1998; Sarachik & Cane, 2010; Straus & Shukla, 2002). A warm or positive ENSO is characterized by the warming of SST, while a cold or negative ENSO is characterized by SST cooling. ENSO impacts are globally felt and include regions of North and South America, Asia, Africa, and Australia. In the United States, a positive ENSO results in wet, cool conditions in the southern

and southeastern states; the Midwest often experiences warm and dry conditions. The opposite is true when a negative ENSO is in phase (Hu & Huang, 2009; Kellner & Niyogi, 2015; Jeffrey C. Rogers & Coleman, 2003; Sarachik & Cane, 2010; Ting & Wang, 1997).

The second climate oscillation is the Atlantic Multidecadal Oscillation (AMO), AMO was first coined in scientific literature in the late 1990s. AMO has an oscillation period of 50 to 70 years and is measured by sea surface temperatures (SST) in the North Atlantic Ocean (Delworth & Mann, 2000; Kerr, 2000; Sutton & Hodson, 2005). It is believed that the thermocline circulation drives AMO (Delworth & Mann, 2000; Dima & Lohmann, 2007). However, Clement et al. (2015) test this hypothesis with inconclusive results, others have linked aerosols as a contributing factor (Booth, Dunstone, Halloran, Andrews, & Bellouin, 2012). The phases of AMO influence the Atlantic hurricane season. A negative AMO reduces the number of hurricanes formed, as well as precipitation, temperature and drought globally (Folland, Palmer, & Parker, 1986; Knight, Folland, & Scaife, 2006; Li & Bates, 2007; Sutton & Hodson, 2005; Trenberth & Shea, 2006). During a positive AMO, the majority of the United States experiences a deficit of rainfall and warmer temperatures resulting in favorable conditions for drought (Enfield, Mestas-Nuñez, & Trimble, 2001; Kam, Sheffield, & Wood, 2014; McCabe, Palecki, & Betancourt, 2004; Jeffrey C. Rogers & Coleman, 2003).

Another climate oscillation originating in the Atlantic Ocean is the North American Oscillation (NAO). NAO is measured by sea surface pressure differences between the Azores High in Lisbon, Portugal and the Icelandic low in Stykkisholmur, Iceland. A small pressure difference is representative of a negative NAO with weaker westerlies. NAO has a shorter oscillation period of only a few years (J. W. Hurrell, 1995; J. W. Hurrell, Kushnir, Ottersen, & Visbeck, 2003; Jeffery C. Rogers & Rogers, 1984; Visbeck, 2002; Wang & You, 2004). NAO

has the most influence on winter weather of Europe, Asia, and the United States. A negative phase of NAO results in warmer and wetter winters with higher streamflow in the Mississippi River Basin (Coleman & Budikova, 2013; Durkee et al., 2008).

The second climate oscillation of relevance for this study that originates in the Pacific Ocean is the Pacific Decadal Oscillation (PDO). PDO's phases are measured from SST anomalies in the north Pacific, characterized by a horseshoe-shaped SST and an oscillation of 40 to 60 years (Deser, Trenberth, & (Eds), 2016; Di Liberto, 2016; Mantua, Hare, Zhang, Wallace, & Francis, 1997; Wen, Kumar, & Xue, 2014). A positive phase is characterized by cool SST in the north Pacific and warm coastal waters near North America (Mantua & Hare, 2002). The forcing behind PDO is relatively unknown and has been hypothesized to be due to ocean memory, currents, and semi-permanent pressure systems (Di Liberto, 2016). PDO has global impacts extending further than North America: Australia, and eastern Asia precipitation and temperature is also impacted (Mantua & Hare, 2002). In the United States, PDO has similar spatial impacts as ENSO, making them difficult to distinguish. PDO impacts are often weaker than ENSO (Deser et al., 2016; Hu & Huang, 2009; Mantua & Hare, 2002; Mills & Walsh, 2013). In Alaska, Neal, Walter, & Coffeen, (2002) found PDO phases to regulate the streamflow, through winter temperatures and precipitation.

The final relevant climate oscillation is the Pacific North American (PNA). PNA also finds its origins in the Pacific Ocean and is influenced by the East Asian Jet Stream and ENSO, having an oscillation period of a few years (Climate Prediction Center Internet Team, 2012; D. J. Leathers & Palecki, 1992; Daniel J. Leathers et al., 1991). In the eastern United States positive PNA is associated with cooler temperatures and slight decreases in precipitation, which impact streamflow, while western Canada experiences warmer temperatures and less precipitation

increasing drought risk (Asong, Wheeler, Bonsal, Razavi, & Kurkute, 2018; Climate Prediction Center Internet Team, 2012; Daniel J. Leathers et al., 1991; Jeffrey C. Rogers & Coleman, 2003).

Climate oscillations do not act independently; they interact to modify their local impacts. PDO and PNA interact with ENSO to alter their spatial and temporal impacts in the United States (Hu & Huang, 2009; D. J. Leathers & Palecki, 1992; Jeffrey C. Rogers & Coleman, 2003). For example, when ENSO and PDO are in-phase, their spatial impacts are intensified, while when out-of-phase, their impacts are reduced (Hu & Huang, 2009). McCabe et al. (2004) utilized Principal Component Analysis (PCA) to explore the relation of AMO, PDO, and northern hemisphere temperatures and their relation to drought. They found together AMO and PDO explain 52% of the drought variation in the continental United States and a positive AMP increases drought with PDO contributing to the spatial patterns observed.

Climate Oscillations and their impacts on crops

Few studies have analyzed multiple climate oscillations and their impacts on crops. Globally, Heino et al. (2018) simulated global crop yields for 12 crops and three climate oscillations. The crop yields were then converted into calories losing the diversity of crop types impacted but showed overall impacts of the oscillations. Regionally, Ceglar et al. (2017) analyzed national winter wheat and maize yields and four oscillations in Europe. They found spatial differences in response to the climate oscillations that have the largest impact during sensitive growing periods. In the Southeast United States, Tian et al. (2015) found that winter wheat yields in the southeast United States were influenced by decadal variations attributed to AMO, PDO, and NAO.

ENSO has also been known to have an impact on human health, fishing, and agriculture. Human health is impacted by promoting favorable conditions for outbreaks of pest, disease and persistent extreme temperature (Kovats et al., 2003; McKinnon, Rhines, Tingley, & Huybers, 2016; Vincenti-Gonzalez, Tami, Lizarazo, & Grillet, 2018). Fishing industries off the coast of South America are impacted by the upwelling of nutrients in the Pacific. Regionally and globally, there have been many studies that have analyzed the impact ENSO has to agriculture crops (Anderson et al., 2018; Gimeno et al., 2002; Heino et al., 2018; Iizumi et al., 2014; etc.). Hansen et al. (1998) and Martinez et al. (2009) find that in the Southeast United States ENSO phase impact maize and tobacco yields.

Compared to the impact studies of ENSO, few studies have analyzed the global impacts of other climate oscillations on crop yields. In the southeast United States, Maxwell et al. (2013) related honey production and tree ring growth to the phase of AMO: low honey production was associated with a positive AMO. NAO influence spring blooming in Norway, NDVI in Europe and northern Asia, maize in Europe and China, and European wheat yields (J. W. Hurrell et al., 2003; Kim & McCarl, 2005; Wang & You, 2004). Wheat in the United States generally experiences an increase in yields under a negative NAO. Maize yield response to NAO varies by state. However, the United States generally experiences a slight increase in yields during a negative NAO (Kim & McCarl, 2005). PDO is often associated with changes in salmon stock in Alaska, western Canada, and western United States, and the onset of spring in western North America (Mantua & Hare, 2002; Mantua et al., 1997). Henson et al. (2017) conducted a regional study in Missouri on the impacts of ENSO and PDO to historical maize and soybean yields; they found the positive phases of ENSO and PDO to increase yields in both crops. Martinez et al.

(2009) found PNA is correlated with maize yields in the Southeast United States, while Jeffrey C. Rogers et al. (1991) found the PNA influences citrus fruit.

Maize and Winter Wheat

Two major crops of the United States will be analyzed for their responses to climate oscillations. The crops are maize, a summer crop and winter wheat a winter crop. Both annual crops are grown predominantly in the study region, and have large economic impacts regionally and globally.

Maize in the United States is primarily planted in May in the Midwest, with earlier planting date further south, and harvested around October (Sacks, Deryng, Foley, & Ramankutty, 2010). The vegetative season is defined as the period between juvenile and adult, where the majority of plant growth occurs (Lauter, Kampani, Carlson, Goebel, & Moose, 2005). The adult stage is defined as when the plant supports reproductive growth features. For maize, the reproductive growth stages, flowering, fruiting, and grain fill, begin in July and continue through September (Hanway, 1963). Winter wheat is primarily planted in October, when little growth occurs, allowing time for winter hardening before the dormant period occurs in the winter months. During spring months, the winter wheat begins growing again and flowering occurs in the reproductive period, with harvest occurring in July (Nleya, 2012; Sacks et al., 2010).

The reproductive period is considered to be one of the most sensitive growth periods (Çakir, 2004; Denmead & Shaw, 1960; Saini & Westgate, 1999). Prolonged exposure to drought conditions can delay flowering, cause pollination failure, and early grain development in both maize and winter wheat with the potential to reduce yields 66% to 90% (Çakir, 2004; Kamara, Menkir, Badu-Apraku, & Ibikunle, 2003; Saini & Westgate, 1999; X.-P. Song et al., 2018).

Photosynthetic ability is reduced, which reduces the Leaf Area Index (LAI), impacting the quality of grain (Mangani et al., 2018).

Flooding can also cause negative impacts to LAI, impacting dry matter in the vegetative and reproductive periods (Mangani et al., 2018). Flooding that occurs prior to planting can force producers to plant later, while flooding after planting can prevent field management reducing yields in maize (Baum et al., 2019). Winter wheat exposed to prolonged flooding conditions causes waterlogging and decreases yield quality and quantity (Luxmoore, Fischer, Stolzy, & N, 1973; Olgun, Metin Kumlay, Cemal Adiguzel, & Caglar, 2008).

Cool air and soil temperatures in the vegetative period of maize can delay development, reduce mineral uptake, and increase pests; the high temperature can cause a decrease in grain filling time length, which reduces the dry weight (Bollero, Bullock, & Hollinger, 1996; J. H. Porter, Parry, & Carter, 1991; Wilhelm, Mullen, Keeling, & Singletary, 1999). Winter wheat is sensitive to temperature at all growth stages. Improper hardening prior to the dormant period can cause winterkill. Warm temperatures during the dormant period can result in winter wheat to come out of dormancy early and become more susceptible to frost; frigid temperatures with little snow cover can result in winterkill (Nleya, 2012; Trnka et al., 2014).

Objectives

Agriculture impacts due to climate oscillations have been analyzed spatially at global and regional levels while ignoring the spatial variability within a region. This thesis focuses on analyzing the impacts at the climate divisional scale in the rainfed regions of the United States. Each climate division has relatively homogeneous climate. The first chapter of this paper will explore the spatial and temporal variability of maize and winter wheat in the United States. This will be accomplished by addressing three objectives: 1) analyze the dominant spatial and

temporal patterns of maize and winter wheat from 1960 to 2016 2) Evaluate crop yield variability attributed to teleconnections with climate oscillations. 3) Understand the predictability of maize and winter wheat yields originating from climate variability. The second chapter will explore the spatial and temporal variability of maize and winter wheat crop failure. There will be two objectives 1) identify spatial patterns of crop failure frequency associated with climate oscillations. 2) Understand the causes of changes in crop failure frequency due to climate oscillations.

Chapter 1

Spatiotemporal patterns of maize and winter wheat yields in the United States: predictability and impact from climate oscillations

(This chapter has published in Agricultural and Forest Meteorology)

Abstract

Studies have shown linkages of climate oscillations with climate extreme events, such as floods and droughts, which may induce risks in summer and winter crop productions. The goal of this study is to explore spatial and temporal variability of a summer crop (maize) and a winter crop (wheat) yields and its linkages with influential climate oscillations in the United States. The county level yield data over 1960-2016 for maize and winter wheat were aggregated into each of the 260 climate divisions in the rainfed regions of the United States, with the linear yield trend being removed. The rotated Principal Component Analysis (PCA) reveals that the first five principle components explain 79% (maize) and 72% (winter wheat) of the spatial and temporal variability of crop anomalies. The first principle component of crop yield variability is strongly associated with the Atlantic Multidecadal Oscillation (AMO). The results of multiple linear regressions for predicting yield anomalies using climate indices show that, climate indices during the reproductive period of maize explained final yield better than the vegetation period (30% versus 26%), while climate indices for winter wheat during the dormant and reproductive growth periods are similar and not significant (25% versus 28%). Categorical yield forecasts using random forecast techniques show that the low (below 30th percentile) and high (above 70th percentile) yields are well predicted by climate indices. Spatially, AMO is identified as the most

important predictor for maize in 46% climate divisions and for wheat in 33% climate divisions.

The results from this study may contribute to understanding the risks of large-scale climate oscillations to local-scale crop production and improving crop yield predictions.

1. Introduction

Climate oscillations influence crop production by modulating seasonal growing conditions for crops. At the global scale, climate oscillations contribute to one-third of the crop yield variability annually, varying across crop types and locations (Ray et al., 2015). A substantial decrease in yield in major food-producing regions, such as the United States, may influence global food security having severe repercussions for regions depending on imports.

Anomalies in temperature and precipitation characterize climate oscillations, a result of large-scale atmospheric-ocean circulations. These large-scale circulations, known as climate modes measured by climate indices, influence global patterns through teleconnections, i.e., the connections of meteorological phenomena among different locations through atmospheric-ocean circulations (Wallace & Gutzler, 1981). For example, El-Niño Southern Oscillation (ENSO), as one of the most well-known climate modes, has significant impacts on local climate conditions and crop yields around the world (Cole & Cook, 1998; Hansen et al., 1998; Henson et al., 2017; Iizumi et al., 2014; Kellner & Niyogi, 2015; Mariotti, 2007). ENSO is measured from sea surface temperature anomalies in the tropical Pacific Ocean and has an oscillation period of 2-7 years (Cole & Cook, 1998; Straus & Shukla, 2002). Iizumi et al. (2014) have shown that the positive, warm phase of ENSO, El Niño, has significant negative impacts on the maize and wheat yields (22%), while also experiencing significant positive soybean and rice yields in the United States, China, as well as other locations globally. Regional studies in the U.S., mainly in the Southeast and Midwest, also found ENSO phases influence crop yield (Hansen et al., 1998; Kellner & Niyogi, 2015; Mourtzinis, Ortiz, & Damianidis, 2016).

Besides ENSO, there are several climate modes that have been identified as influential on local climate conditions in the United States as well as other regions of the world, including

Atlantic Multidecadal Oscillation (AMO), North American Oscillation (NAO), Pacific Decadal Oscillation (PDO), and Pacific North American (PNA) oscillation. AMO has an oscillation period of 60-70 years, sea surface temperatures in the North Atlantic Ocean determine its phase (Kerr, 2000; Sutton & Hodson, 2005), driven by the thermocline circulation (Delworth & Mann, 2000; Dima & Lohmann, 2007). Globally, AMO impacts various climate and weather conditions experienced from Europe to Brazil. AMO phase influences Atlantic hurricane activity (Knight et al., 2006; Trenberth & Shea, 2006) and precipitation trends (Enfield et al., 2001; McCabe et al., 2004). Similar to AMO, NAO also has its origins in the Atlantic Ocean and is measured by sea level pressure differences between the Azores High and Icelandic low (Dahlman, 2009; J. W. Hurrell, 1995; Wang & You, 2004). NAO phase predominantly influences winter conditions in Europe and the United States (Kim & McCarl, 2005; Visbeck, 2002). Sea surface temperature anomalies in the North Pacific Ocean define PDO (Deser et al., 2016); the positive phase is characterized with cold waters in the North Pacific Ocean and with warm coastal waters along western North America the opposite is true for the negative phase (Di Liberto, 2016; Wen et al., 2014). A phase of PDO can persist for 20 to 30 years (Mantua & Hare, 2002). Australia, Brazil, China, and North America experience changes in the onset of spring, temperature, and precipitation associated with PDO phases (Mantua & Hare, 2002; Neal et al., 2002). In the United States, PDO's spatial pattern of precipitation and temperature is similar to ENSO, except that correlation values associated with PDO tend to be weaker (Mantua and Hare, 2002). The other influential climate mode is PNA, which originates from the North Pacific region and is influenced by the East Asian Jet Stream and ENSO (Climate Prediction Center Internet Team, 2012). The strongest influences of PNA (both precipitation and temperature) occur over North

America during the winter months (Asong et al., 2018; Climate Prediction Center Internet Team, 2012; Daniel J. Leathers et al., 1991).

Climate modes have also been shown to interact with each other, influencing the local conditions experienced. McCabe et al. (2004) analyzed northern Hemisphere temperatures, AMO, and PDO relation to drought through rotated Principal Component Analysis (PCA) and correlations. They found that PDO and AMO explain 52% of the variation of drought in the continental United States, positive AMO increases drought frequency while PDO phase contributes to the spatial patterns of drought. PDO and PNA interact with ENSO to modify spatial and temporal connections, thus altering the expected seasonal weather (Hu & Huang, 2009; D. J. Leathers & Palecki, 1992; Jeffrey C. Rogers & Coleman, 2003). An example of this is when ENSO and PDO are in phases their impacts may be strengthened and when out of phases their impacts may be weakened (Hu & Huang, 2009).

Impacts of climate modes on crop productions are mainly from ENSO, either in the United States (Hansen et al., 1998; Henson et al., 2017; Kellner & Niyogi, 2015; Mourtzinis et al., 2016), and globally (Heino et al., 2018; J. W. Hurrell et al., 2003; Iizumi et al., 2014). Connections between other climate indices and crop yields have been identified regionally across the globe. For Europe, Ceglar et al. (2017) identified strong links between country-averaged crop yields in Europe and NAO, Eastern Atlantic (EA), Scandinavian (SCAND) and Eastern Atlantic-Western Russia (EAWR) patterns. For the southeastern United States, Tian et al. (2015) found decadal oscillations in simulated winter wheat, were connected with AMO, PDO, and NAO oscillations. Maxwell et al. (2013) concluded that tupelo honey production in the panhandle of Florida is inversely related to the AMO phase. Globally, NAO was identified as influential on simulated crop productivity in Europe, the Middle East, the United States as well as other

countries around the world (Heino et al., 2018). During the negative NAO phase, Europe usually endures a decrease in wheat and maize yields whereas the United States witnesses the opposite (J. W. Hurrell et al., 2003; Kim & McCarl, 2005). Henson et al. (2017) found in Missouri PDO and ENSO interact with each other to influence the climate conditions experienced during summer growing season and yield anomalies of maize and soybeans. Martinez et al. (2009) discovered that PNA affects maize yield in the southeastern United States.

Although connections between food production and climate oscillations have been explored at regional or global levels, spatial variability within large countries such as the United States, where the effects may be substantial, have been neglected in previous studies. The overall goal of this study is to explore spatial and temporal variability of summer (maize) and winter (wheat) crop yields and their linkage with climate oscillations at the climate-division scale in the rainfed regions of the United States. This study is the first to analyze spatial-temporal patterns of crop yields and their predictability and impacts from climate oscillations at the climate division scale. There are three specific objectives in this study: 1) analyze the dominant patterns of spatiotemporal variability of both summer (maize) and winter (wheat) crop yields using PCA, 2) explore if crop yield variability are attributed to teleconnections with the modes of climate oscillation, and how much is the variability due to modes of climate oscillation, and 3) assess the ability of using climate indices to predict crop yield anomalies and categories. The knowledge gained in this study will be helpful for understanding spatiotemporal variability and predictability of crop yields originated from climate oscillations and will provide useful information for improving crop yield forecasts and climate risk management in agriculture.

2. Data and Methods

2.1 Study Region

The study focuses on the climate divisions over rain-fed regions (east of the 100° W Meridian) of the United States (Figure 1.1), where nearly 90 percent of the agricultural lands are rainfed (NASS, 2014a, b). We selected this region in order to minimize effects from irrigation since prevalent irrigation may offset the impact of climate on crop yields (Ceglar et al., 2017). In our study region, areas of prevalent irrigation include east-central Nebraska, western Kansas, the panhandle of Texas, eastern Arkansas, and southwest Georgia. Since the study region experiences dramatic regional differences in climate, analysis based on climate divisions will provide a more accurate representation of climate-induced spatial variability within the region. The study region covers 260 climate divisions with each climate division having relatively homogeneous climate conditions (Karl & Riebsame, 1984).

2.2 Crop yield data

Annual crop yield and production data for maize and winter wheat in each county in the study region over 1960 to 2016 were obtained from the National Agricultural Statistic Service (NASS) of United States Department of Agriculture (USDA) (via: <https://quickstats.nass.usda.gov/>). These two crops were chosen because they are the most important summer and winter crops, respectively. Yield data was processed by taking weighted averages of county-level yield data over each climate division of the study region, using county production as a weight. Climate divisions with fewer counties reporting NASS yields will result in less robust yield averages. Therefore, we assume that the resulting climate division yields are homogenous. To ensure that the crop yield data are temporally and spatially complete, we conducted a simple quality control and pre-processing process. First, we removed climate

divisions missing more than 70% of their yield data. The remaining gaps were then filled using two procedures as follows. The first procedure fills the gaps using a moving median with a window of 10 years. The second procedure uses K-Nearest Neighbors (KNN) Imputation, where missing values were calculated using the mean of nearest neighbors, to fill the remaining gaps (Johnson & Wichern, 2008; Troyanskaya et al., 2001). After the quality control and pre-processing procedure, 5-year moving average was conducted for annual crop yields over each climate division to smooth out the short-term variability, since the climate modes analyzed in this study typically have more than 5-year oscillation period. The crop yield time series for each climate division was then de-trended using a linear trend to remove and limit the effects of technology and farming practice advances over time, including irrigation. The crop yield data after removing the trend is called crop yield anomalies. This entire process resulted in a temporally and spatially complete 5-year average maize yield anomalies over 1960 to 2016 at 240 climate divisions, and winter wheat yield anomalies over 1967 to 2016 at 222 climate divisions (Figure 1.2).

2.3 Climate data

Modes of climate oscillations are represented by climate indices. Influential climate indices considered in this study include AMO, ENSO, NAO, PDO, and PNA. Monthly indices were obtained via the internet as follows: the Physical Sciences Division of the Earth System Research Laboratory for AMO (<https://www.esrl.noaa.gov/psd/data/timeseries/AMO/>) and ENSO (<https://www.esrl.noaa.gov/psd/data/correlation/nina34.data>). Monthly data for NAO index was obtained from the Climate Analysis Section of the National Center for Atmospheric Research (J. Hurrell & National Center for Atmospheric Research Staff, 2017). Data for the PDO index was retrieved from the Joint Institute for the Study of Atmosphere and Ocean at the

University of Washington (<http://research.jisao.washington.edu/pdo/PDO.latest.txt>). PNA values were obtained from the Climate Prediction Center Internet Team of NOAA (http://ftp.cpc.ncep.noaa.gov/wd52dg/data/indices/pna_index.tim). Surface climate variables data including maximum and minimum temperature (T_{\max} and T_{\min}), precipitation, and Palmer Drought Severity Index (PDSI) for each climate division were obtained from the National Climatic Data Center (NCDC) at: <https://www.ncdc.noaa.gov/monitoring-references/maps/us-climate-divisions.php>. Surface climate data for each climate division are the monthly mean of the observed variable over the weather stations within a climate division.

In order to account for crop growth sensitivity to climate conditions throughout various phases in the growing season (Mourtzinis et al., 2016), the growing season has been divided into different growing periods according to planting and harvest dates in Sacks et al. (2010). The growing season of maize was divided into vegetation period (April, May, June) and reproductive period (July, August, September), as in previous studies (Berglund, Endres, & McWilliams, 2013; Iizumi et al., 2014). Winter wheat was divided into vegetation (September, October, November), dormant (December, January, February, March) and reproductive (April, May, June), as in previous literature (Hall & Nleya, 2012; Iizumi et al., 2014; Nleya, 2012; Sacks et al., 2010). Since winter wheat during the vegetation period is limited to seedling growth (Nleya, 2012), before the dormant period, the vegetative period for winter wheat was not included in the analysis. Climate indices and surface variables were averaged over each growing period, which accounts for the time lag in the atmosphere (Iizumi et al., 2014). Similar to crop yields, a 5-year moving average was applied to the climate indices and surface climate variables.

2.4 Data analysis

Dominant patterns of spatiotemporal variability of maize and winter wheat yields were analyzed using PCA with a varimax rotation. The relationships between the principal components (PC) of crop yields and the climate indices were analyzed using correlation analysis. The variability of crop yields induced by climate oscillations were evaluated in each climate division using multiple linear regressions with the climate indices as independent variables and the crop yield anomalies as dependent variables. Categorical yield prediction was produced using the random forest technique with climate indices as predictors. The performance of categorical yield prediction was evaluated using Brier score. A detailed description of each analysis is given below.

2.4.1 Exploring dominant patterns of the crop yields using PCA

The processed dataset of crop yields can be considered as a matrix with m (number of climate divisions) columns and n rows (number of years). PCA, also referred as Empirical Orthogonal Function (EOF) analysis, is a classical technique for dimensionality reduction, which has been widely used in climate research to study possible spatial modes (or patterns) of variability and how they change with time (e.g. McCabe et al., 2004). Detailed description of PCA method has been given in a number of textbooks (e.g. Johnson and Wichern, 2008; Wilks, 2011). Briefly, PCA can reduce a dataset containing a large number of variables (in this case, crop yield data matrix) to a dataset containing fewer new PCs (in this case, PCs of crop yields). PCA is mathematically defined as an orthogonal linear transformation that transforms the original data to a new coordinate system such that the greatest variance by some projection of the data comes to lie on the first PC, the second greatest variance on the PC, and so on. Specifically, the PCs are linear combinations of the original ones, and a number of PCs (p) are chosen to

represent the maximum possible fraction of the variability contained in the original data, so that the most amount of variation is explained by the number of retained PCs with $p \ll m$. The transformed values corresponding to each data point is called PC scores. The coefficient for each of the original variable in the linear combination equation is called loading. The eigenvalue of the correlation matrix of the original data matrix, defined as λ_k , is the variance explained by each PC. In this work, we used scree plot criteria to determine the final number of PCs to retain (Wilks, 2011). Through PCA reduction, the original data matrix is then transformed from m climate divisions times n years of crop yields to p number of PCs times n years of PC scores. The varimax rotation were applied to the retained PCs to achieve simple structures and improve physical interpretability by making the large loadings larger and small loadings smaller. The resulted PC scores and loadings allow: i) capturing the dominant patterns (or modes) of temporal (with PC scores) and spatial (with loadings) variability in the crop yields, and ii) comparing these dominant patterns with climate data to explore any plausible relationships.

2.4.2 Analyzing relationships between principal components of crop yields and climate indices

Linear correlations were performed to identify significant relationships between climate indices and PCs of crop yields. Correlation to determine association between two variables is utilized in many climate studies (e.g. Martinez et al. 2008; McCabe 2004). It is important to note that correlation does not give causations or physical processes between variables, rather correlation provides the strength of the association between variables. The student- t test was used to determine significance of the correlations. Autocorrelation is present in time series data due to present and future values dependence on past values; a Monte Carlo technique is also used to more determine significant correlation values. The Monte Carlo technique involves computing the correlation multiple times with a randomized sample of a climate index, constructing a

histogram from the correlation values and determining significance from the histogram (Livezey & Chen, 1983). The Monte Carlo simulation was passed an unsmoothed climate index that was then randomized, a 5-year moving average was applied before being correlated with the PC scores. This process was repeated for 20,000 iterations, significance was determined at the 95th percentile.

2.4.3 Predicting crop yield anomalies using climate indices

Multiple linear regressions are used to predict crop yields using climate indices at each climate division. The model is written as:

$$Y = \gamma_0 + \sum_i \gamma_i \cdot X_i + \varepsilon$$

where $X_{i,t}$ represents independent variables (AMO, PDO, NAO, ENSO, and PNA) over a growing period and ε_t is the error term.. The adjusted coefficient of determination (R^2) is calculated to assess the quality of the regressions and what portion of the variation is explained by the predictors (climate indices).

2.4.4 Predicting crop yield categories using climate indices

To investigate the predictability of yield categories, crop yield anomalies are converted into categories (i.e. low yield, normal yield, high yield) based on percentiles. The lower 30th percentile was represented as low yields; the middle 30th to 70th percentile is defined as normal yields; the upper 70th percentile is defined as high yields. Random forest, as a decision tree type of approaches, provides an ideal tool for predicting yield categories. Random forest is an enhanced decision tree model based on ensemble machine learning algorithms (Breiman, 2001). It operates by constructing multitude of decision trees at training period using bootstrapped resamples of the total datasets and determining the final output by averaging or majority voting of the ensembles of the decision trees (see Brieman, 2001 for details). Assuming that we have a

matrix with n observations and p variables. The random forest algorithm (Liaw & Wiener, 2002) creates B random bootstrap samples of length n by resampling the original data set. A tree is then formed, using m number random predictors (climate indices during reproductive phase) at each node, where the best predictors are chosen. This process is repeated until B number of trees is reached. Each tree will cast a vote contributing to the best categorical yield result, creating voting proportions. The voting proportions will contribute to probabilities used to assess the quality of using climate indices as predictors of the yield category.

The random forest generated probabilities, y_{ki} , for event category i in year k ($k=1, 2, \dots, n$), allowed us to calculate the Brier Score for each event. The Brier Score is a measure of the accuracy of the forecast and is the mean squared error of the probability forecast (Wilks 2011). The events are broken into binary events of occurring $o_i = 1$ and $o_i = 0$. The formula for calculating the Brier score is:

$$BS_i = \frac{1}{n} \sum_{k=1}^n (y_{ki} - o_{ki})^2.$$

Brier score values range from 0 to 1 where 0 indicates an accurate forecast.

3. Results and Discussion

3.1 Patterns of spatial-temporal variability of crop yields

Five PCs for maize and winter wheat were selected according to the scree plot criteria, which explain 79% and 72% of the total variability respectively. After varimax rotation, PC1 explains 28% (18%) of the total variance for maize; PC2 explains 20%; PC3 explains 11%; PC4 explains 12%; and PC5 explains 8% of the total variance (Table 1.1). The variance explained by the PCs for winter wheat is found in Table 1.1. The PC score time series provide a temporal view

of the change in the PCs with time, and the loadings illustrate the spatial distribution of climate division's response to the PC scores.

We further examine each PC score and its associated loadings to reveal the dominant patterns of temporal and spatial variability of maize (Figure 1.3) and wheat (Figure 1.4), respectively. As shown in Figure 1.3, for maize, the PC1 score has less variability when compared to the other PC scores. There is only one maximum in the mid-1980s and a minimum near 2010. The score of PC2 and PC3 both oscillate with small amplitude until the mid-1990s when the amplitudes increase greatly. PC4 has less internal variability than PC5, both having a maximum near 2000. The loadings for PC1 have a positive to negative trend from west to east. High positive values are present in western Kansas and western Texas, while the lowest negative values are in southern Georgia, and northern Florida. Since these areas react strongly from the scores at large magnitudes and if PC scores are correlated significantly with climate indices, it is likely that these areas will result in stronger correlations. PC2 score is mainly composed of loadings ranging from -0.08 to 0.09 the highest positive value is located in western Virginia with values of decreasing magnitude into eastern Virginia. The lowest negative value is in southern Arkansas. The loadings of PC3 are mostly negative, with a few climate divisions respond positively in the south and mid-west regions. The PC4 loadings are consistently positive from southern Midwest into the Gulf States, negative values run from the east coast and into the central Midwest. The PC5 loadings are consistently positive in the upper Midwest and mostly negative in the southern and eastern regions with only a few distinctive patterns.

Figure 1.4 shows a time series of PC scores and the associated loadings in space for winter wheat. In general, the PC scores for winter wheat have a smaller amplitude than those for maize have, suggesting that the winter wheat yield is less variable in time than maize yield. The

score for PC1 includes two 20-year oscillations in the time period. The amplitude of PC2 score increases as the time series progresses, the largest increases occurring after 1990. PC3 score has a smoother longer curve only one oscillation is fully completed, internal variability is present around the 2000s. Similar to PC3 score, the score of PC4 has a prolonged oscillation period. The scores of PC4 and PC5 have more internal variability than PC3 score. Present in PC5 score is a similar, but opposite trend as PC4 score. The loadings for PC1 of winter wheat have a mixture of negative and positive values that run horizontally across the study region and two regions is higher positive values around the Great Lakes and Mississippi Delta regions. The PC2 loadings show higher values from the southwest tip of Missouri to Ohio surrounded by regions of lower values. The highest positive value of all winter wheat PC loadings is located in west Texas for PC4. Loading PC4 has a region of high positive loading values observed near Kentucky and Tennessee. A negative loading region is present in Nebraska and Kansas for PC5. The surrounding regions vary between small positive and negative except for northern Wisconsin where there is a larger loading value.

3.2 Correlations between principal components of crop yields and climate indices

Figure 1.5 shows correlations of climate indices with PCs of maize and winter wheat yields during the vegetative and reproductive periods (Figure 1.2). Correlations between PC1 for maize and AMO show the highest values during vegetative and reproductive periods ($|r| \geq 0.67$). The next highest correlation $r = 0.63$ with PNA may be due to smaller internal variability. PC2 and PC3 have lower correlation values $|r| < 0.30$. The high correlation ($|r| > 0.47$) between PC4 and PDO may be a result of the long oscillation present in the score of PC4. While the correlation between PC4 and ENSO may be a result of spatial similarities. PC5 correlation

values for indices originating in the North Pacific Ocean (PDO and PNA) are stronger than the Atlantic Ocean Indices (AMO and NAO).

Correlation values for PC1 and PC3 of winter wheat are nearly opposite in sign, and this is also present in the scores of PC1 and PC3 (Figure 1.4). For both PC1 and PC3, AMO has the highest correlation ($r > 0.48$) and may be a result of the longer trends in scores of PC1 and PC3 seen in Figure 1.4. PC1 and PC3 show weaker correlation values ($r < 0.38$) with shorter term climate indices. PC2 has many weaker correlations with the highest correlation values ($0.30 \leq |r| \leq 0.39$) occurring in the vegetative phase from climate indices originating in the North Pacific Ocean. The highest correlation ($r = 0.43$) of PC4 in the vegetative phase occurs with AMO while in the reproductive phase PNA has the highest correlation value ($r = 0.48$). Correlation values in the vegetative phase of PC5 are similar, while those in the reproductive phase show more variability ($0.14 \leq |r| \leq 0.63$). The reproductive phase ENSO and PDO have correlation values, $r = 0.60$, with PC5 suggesting they contribute equally to yield variability. The seasonal timing of the reproductive periods for maize and winter wheat likely plays a role in the yield response to precipitation. The reproductive period of maize occurs during summer months when convective systems dominate the spatial variation and amount of precipitation received (Daly et al., 2008; Fritsch et al., 1986), while winter wheat's reproductive period occurs earlier in the year when there is a higher soil moisture content (Hollinger, Isard, Hollinger, & Isard, 1994).

Due to the reduced degrees of freedom, a standard two-sided t -test at a 95% significance level will result in several modes being significant with each PC. Figure 1.5 shows significant indices indicated by an asterisk (*). In general climate indices with higher correlations ($|r| \geq 0.25$) resulted in significant correlations. Both PC2 and PC3 for maize and winter wheat had the least

amount of significant correlations, consistent with the lower correlation values. These PCs may represent other factors that are influencing yields, such as disease and pest.

Due to autocorrelation in time series data, a Monte Carlo shuffling technique is also used to determine significant correlation values, which results in a reduced number of significant correlations by *t*-test. Correlations that were significant via the test using the Monte Carlo method are circled in Figure 1.5. The Monte Carlo test result shows that AMO is significantly correlated negatively with PC1 of maize during both vegetative ($r = -0.67$) and reproductive periods ($r = -0.70$). AMO is positively correlated with PC1 of winter wheat during the dominant period ($r = 0.64$). The correlation between PC1 and PNA ($r = -0.63$) is only significant for the reproductive period of maize. For both maize and winter wheat, neither PC2 nor PC3 is significantly correlated with any climate indices. For maize, PC4 is significantly positively correlated with ENSO during the reproductive period ($r = 0.47$), and PC5 is significantly correlated negatively with PNA during the vegetative period ($r = -0.52$). For winter wheat, PC5 is significantly correlated negatively with ENSO and PDO during the reproductive period $r = 0.61$ and $r = 0.63$, respectively.

Time series of PC scores of maize and winter wheat are plotted against significantly correlated climate indices according to the *t*-test and Monte Carlo methods in Figure 1.6. The trend lines for AMO of the maize vegetative and reproductive periods follow a similar trajectory as PC1 score, with AMO leading the score. PC1 score may, therefore, be associated with AMO as they both have long-term trends. PC4 score and reproductive ENSO are positively correlated. PC4 captures the general trend but fails to fully capture the smaller variability of the ENSO oscillation. PNA during maize vegetative period leads PC5 score prior to mid-1990s; however this trend reverses in later years. Suggesting that PC5 score may be associated with shorter term

variability, as explained by PNA earlier in the time series, however other factors may influence the time series in later years. In Figure 1.6, the temporal plots of winter wheat, PC1 score, and AMO during the dormant period are positively correlated and show a similar long-term trend. Similar to maize PC1 score and AMO temporal plots, AMO leads the general trend. PC1 score and AMO during the reproductive period had a relatively large positive correlation (0.57), which indicates that PC1 score for winter wheat is also associated with long-term variability. PC5 score is significantly correlated with ENSO and PDO (reproductive phase), this may be a result of ENSO and PDO having similar temporal and spatial trends at the beginning and end of the observation period (Mantua et al., 1997). PC5 score may be associated with sea surface temperatures in the Pacific Ocean as both ENSO and PDO originated in the Pacific Ocean (Di Liberto, 2016).

Correlations between the climate indices and crop yields are plotted in Figure 1.7. The reproductive period for maize has stronger correlation values than that of the vegetative period, agreeing with previous research that the reproductive period plays an important role in determining yield (Mourtzinis et al., 2016). For winter wheat, smaller differences in correlation between reproductive and dormant periods are observed. The analysis of these results in regions of high irrigation, such as Nebraska and western Texas, should be viewed with caution. Irrigation can act to mitigate the effects of drought and high-temperature effects on crops (Ceglar et al., 2017; Jones, Hansen, Royce, & Messina, 2000).

The spatial patterns of the effect of AMO on maize (both vegetative and reproductive periods) and winter wheat (dormant period) are closely related to the spatial pattern of loadings for PC1 of maize and winter wheat. Consistent with the correlations between AMO and the PC1 of maize and winter wheat, spatial patterns are opposite for maize and agreeing for winter wheat.

(Figure 1.3, Figure 1.4). These findings further support the findings that PC1 is related to long term variability of crop yield. Winter wheat yield and indices correlations of ENSO and PDO both exhibit similarities, the Gulf States and the Great Plains, in their spatial distributions (Hu & Huang, 2009; Mantua et al., 1997). These spatial similarities are also presented in PC5 loading, further solidifying the earlier conclusion that PC5 of winter wheat yields is associated with ENSO and PDO.

3.3 Responses of crop yields to changes in phases of climate indices

We further look at the responses of crop yields to the changes in phases of each climate index over each climate division, by calculating the difference between the average divisional yields during the upper tercile and the lower tercile of each climate index. A *t*-test was utilized to evaluate if the difference in yields are statistically significant at 95% level. The results of these differences and significance for both maize and winter wheat are shown in Figure 1.8.

Significant maize yield differences, for all climate indices, were more likely to be experienced in the Great Plains through Texas and the Gulf States. While the Northeast through the Midwest have smaller differences with fewer regions of significance, these patterns may be attributed to particular elements of the climate indices. For example, AMO (Figure 1.8, Maize A.) shows significance in the Great Plains region may be attributed to the changes in precipitation which also caused changes in streamflow as noted by Enfield et al. (2001). The larger difference observed in the Western Plains and the Southeast coincide with the largest loading values of PC1, which indicates yields in these regions are more sensitive to AMO index changes and further confirms that PC1 is associated with yield variability driven by AMO. NAO has few areas of significant correlation and may be a result of NAO being more prominent in the winter months (Coleman & Budikova, 2013), and a longer lag is needed to see effects in the

reproductive growing period. Our results differed from Kim and McCarl (2005), particularly in central Midwest where Kim and McCarl indicate a change in maize yields between phases. However, there is an agreement in western Nebraska through Northern Texas. ENSO resulted in a difference of yield in all regions but the Midwest and parts of the East Coast. The region that results in the largest change in yields are portions of the Gulf States through the eastern portions of the Great Plains region, which is consistent with the largest impacts as indicated by Iizumi et al. (2014). Regions of significant yield difference under different phases of PDO (PNA) correspond well with regions of high PDO (PNA) yield correlations (Figure 1.7). Further, reinforce that these regions are experiencing yield differences as a result of PDO (PNA) phase.

The spatial patterns of winter wheat yield differences were more variable and covering larger spatial areas compared to that of maize; this may be a result of climate indices having a larger magnitude index in winter months progressing into early springs and summer influencing the reproductive stages of winter wheat. Our results of AMO, NAO, and PDO influencing winter wheat yield are consistent with Tian et al. (2015) who noted the influences in the southeastern US. Shorter oscillation indices, like NAO, varies by location and its impacts may be a result of the index time period being analyzed. When the crop yield is strongly correlated with an index (Figure 1.7) and shows a significant difference in yield (Figure 1.8) provides evidence that the mode may be influencing yield in these regions, thus resulting in these regions being more susceptible to indices phase differences.

3.4 Discussing Plausible causations of crop yield patterns due to climate oscillations

To explore the plausible causations of crop yield patterns due to climate oscillations, we compare correlations between crop yields and significant climate indices (Figure 1.7) with correlations between surface climate variables (precipitation, temperature, and PDSI drought

index) and climate index (Figures 1.9 and 1.10). By comparing and analyzing these correlations, we can hypothesize what may be factoring into a yield decrease or increase for an area.

AMO is significantly correlated with PC1 of maize yield in both the vegetative and reproductive growing periods. Previous studies have linked AMO with drought conditions that occur in the positive phase (Enfield et al., 2001; McCabe et al., 2004; Jeffrey C. Rogers & Coleman, 2003) and an increase in temperature (Sutton & Hodson, 2005). In combination or alone, the changes in drought or temperature may reduce the maize yield. The drought conditions are likely to cause maize yield reductions during water sensitive various growth stages (Çakir, 2004; Denmead & Shaw, 1960), while the higher temperatures cause a reduction in grain weight and yield during the vegetative and reproductive periods (Mourtzinis et al., 2016; Wilhelm et al., 1999). An example of this combination may be occurring in southern Nebraska and northern Kansas where a negative correlation between AMO and yield is present (Figure 1.7), positive correlations with temperature (warmer temperatures with a positive index) (Figure 1.9), and a negative correlation with PDSI (decrease in PDSI with a positive index) (Figure 1.9).

Similar to AMO, PNA was also significant and negatively correlated for the vegetation and reproductive periods of maize (Figure 1.5). The cooler temperatures associated with positive PNA during the vegetative period may delay developmental grow and the onset of the reproductive period (Bollero et al., 1996). PNA has little effect on the temperature for the central United States during the reproductive period and exhibits a positive correlation in the southern Gulf States, this warming in combination with less precipitation causes the decrease of the PDSI values (Figure 1.9). We would expect to see a decrease in yield with positive PNA conditions. However, this is not the case in all locations of the study regions, for example, north Minnesota experiences an increase in yield (Figures 1.7 and 1.8) suggesting that the deviations in climate

variable experienced are not significantly impacting the crop. The negative correlation between PNA and yield in Texas may be explained by the increase in temperatures and the negative PDSI values, despite the minimal positive correlation with precipitation.

ENSO is positively correlated with yields in the reproductive period of maize (Figure 1.7). The increase in yields through the southeast may be a result of wetter conditions during the reproductive period (Figure 1.9) resulting in fewer stress days on the crop. The northern Great Plains region is likely to experience a decrease in yield, which may be a result of the decrease in maximum temperature and increase precipitation. These combined climate conditions provide more favorable conditions for fungi and crop diseases. Texas and the southern plains experience both positive and negative correlations in yield (Figure 1.7), thus highlighting the uncertainty and variability in the region despite near consistent correlations (Figure 1.9). Regionally, increases in temperature and decreases in precipitation can cause both increases and decreases in yield during a positive ENSO event. Other factors, such as hail events (Allen, Tippett, & Sobel, 2015) may be contributing to variability.

AMO during wheat's dormant period is positively and statistically significantly correlated with winter wheat yields (Figure 1.5). The conditions that AMO produces can impact winter wheat both positively and negatively. Warmer temperatures can prevent winter kill due to extremely cold temperatures but could also prevent the vernalization process (Nleya, 2012). North Dakota and South Dakota are associated with an increase in yield while also experiencing colder temperatures and more precipitation with a positive AMO event (Figure 1.10); this may be a result of the precipitation in the form of snow and acting as an insulator for the wheat to prevent the cold temperatures from killing the dormant wheat (Nleya, 2012).

The reproductive period of ENSO and PDO are both correlated significantly with PC5 for winter wheat. ENSO and PDO are known to have similar spatial patterns and interact, with PDO driving the intensity of ENSO (Hu & Huang, 2009; Mantua et al., 1997). Both modes are correlated negatively with maximum temperature resulting in cooler temperatures for the majority of the study region but warmer temperatures for the East coast. Warmer temperatures above wheat's optimal temperature may decrease the grain weight (J. R. Porter & Gawith, 1999). Precipitation is positively correlated with the climate indices in southern portions of the study region and negatively correlated in the north.

ENSO index is positively correlated with both maize and winter wheat yields, contrasting previous research indicating an El Niño event results in a yield reduction (Hansen et al., 1998; Iizumi et al., 2014; Martinez et al., 2009). This may be a result of the 5-year moving average which reduces the signal of an El Niño/La Niña event, resulting in more neutral years. Neutral years frequently have higher yields than ENSO events (Iizumi et al., 2014; Kellner & Niyogi, 2015), resulting in a positive correlation.

3.5 Predicting crop yield anomalies and categories using climate indices

Linear regressions were developed to predict crop yields for all the climate divisions in the study area and to explore how much variability of crop yield anomalies is explained by AMO, NAO, ENSO, PDO, and PNA. The regressions were developed by using detrended 5-year moving average yields as the dependent variable and 5-year moving average AMO, NAO, ENSO, PDO, and PNA during different growing periods as independent variables. Figure 1.11 shows the adjusted determination of coefficients (adjusted R^2) of the multiple linear regressions. The estimated winter wheat yields showed higher adjusted R^2 values than maize yields, concurring with Ceglar et al. (2017). For maize, the adjusted R^2 is higher for yield estimates

using climate indices during vegetative period than during the reproductive period, indicating the more prominent effects of climate on maize yields during the former period than during the latter period, as is found in previous studies (Ceglar et al., 2017; Mourtzinis et al., 2016). For wheat, the adjusted R^2 is higher for yield estimates using climate indices during the reproductive period than during the dormant period, confirming with the previous findings showing stronger effects of climate on wheat yields during the reproductive period than during the vegetative period (Ceglar et al., 2017). It is worth noting that the median (mean) adjusted R^2 values for estimating maize and winter wheat using climate indices during the reproductive period are equal to 30% (28%), respectively, indicating that, on average, approximately 30% and 28% of the temporal variability in maize and wheat yields for the climate divisions are explained by the AMO, NAO, ENSO, PDO, and PNA.

Yield categories were predicted using climate indices with the random forest technique at each climate division. Brier score was used to evaluate the performance of the categorical predictions. Brier Score values of maize and winter wheat ranged from 0.041 to 0.327. High and low categorical yield performed better than average yield, low categorical yield has the lowest mean Brier score. Spatial representation of maize and winter wheat Brier are illustrated in Figure 1.12. Maize climate divisions experienced a higher Brier Score from the Midwest to the Appalachians, and a few coastal states climate divisions. The mean Brier Score for high maize yields is 0.162, average yields 0.230 and low yields 0.161. Winter wheat Brier scores values have more variability in Missouri, Kansas, Oklahoma, and Texas. The mean Brier Score for high winter wheat yields is 0.161, average yields 0.227 and low yields 0.158.

The random forest algorithm provided a variable importance ranking for all of the climate divisions (Table 1.2), Rank 1 being the most important variable. Rank 1 for 62% of the climate

divisions for maize is AMO or PNA; this is consistent with our previous PC results in which PC1 is significantly correlated with AMO. Rankings 2 through 4 modes ENSO, PDO and PNA have similar contributions for predicting categorical yield. NAO was the least important variable for 58% of the climate divisions, consistent with the results of the *t*-test where NAO (reproductive) was only significant for score PC5. Spatial patterns of climate division having AMO or PNA are present in Ranking 1, smaller groupings (four climate divisions or less) are present in Rankings 2 through 4, with Ranking 5 having large clusters of NAO as the least important variable. AMO and PNA were the highest ranking variables for winter wheat. Both modes had significant correlations with PC1 score when using a *t*-test (Figure 1.6). The most common ranking for ENSO is Rank 5 (27% of climate divisions), and PDO's is Rank 3 (26% of climate divisions). NAO and ENSO were least important in determining the categorical yield of winter wheat for the climate divisions. Spatial patterns were not as prevalent in winter wheat variable ranking with mode importance being sporadic.

4. Conclusions

In conclusion, this study shows that five rotated principal components explain over 70% of the variance in the 5-year moving average of maize and winter wheat yields in the rainfed regions of the United States. For maize crop, the first component, which explains 28% of total variance, is highly correlated with AMO during both vegetative and reproductive periods and PNA during the reproductive period. The first, fourth, and fifth components, which in total explained 48% of total variance, are highly correlated with one or more climate indices, including AMO, PDO, ENSO, and PNA during either vegetation or reproductive period. Since the second and third principal components are not highly correlated with any climate index, they may represent a complex variability due to other factors than climate oscillation. Winter wheat

yields, which are also highly associated with climate indices, show different patterns compared to maize. The first and fourth principal components, which explain nearly equal proportions of variance (i.e. 18% and 20% respectively), are highly correlated with AMO and PNA during the dormant or reproductive period. The third and fifth components, which in total explain 21% of total variance, are highly correlated with AMO, PDO, ENSO, or NAO during either dormant or reproductive period. Only the second principal component is not highly correlated with any climate index and may represent a complex variability due to non-climate factors. In total, for wheat, 51% of total variance is highly correlated with one or more of the climate index.

Crop yields are indirectly influenced by climate oscillations through modulating surface climate variables. Prolonged exposure to warmer temperatures and drought conditions from AMO reduces yield in maize by stressing the crop, cooler damp conditions resulting from ENSO can reduce yield by promoting disease. Winter wheat is influenced by the temperatures produced from AMO, while ENSO and PDO have similar effects on winter wheat yield. The inclusion of all climate indices, AMO, NAO, ENSO, PDO, and PNA, appears to be crucial in developing multiple linear regressions and random forests that can accurately predict crop yield anomalies and categories both spatially and temporally. Variable importance for maize is spatially dependent for the most important and the least important variables. Winter wheat variable importance is not as defined as it is for maize; however spatial patterns still exist. Models generated from random forest perform well for the upper and lower 30th percentile of yield. This knowledge could be potentially useful to improve crop yield forecasting and climate risk management in United States agriculture.

Table 1.1 The explained variance of the five rotated principle components.

Principal Component	Explained Variance (%)	
	Maize	Winter Wheat
PC1	28	18
PC2	20	13
PC3	11	12
PC4	12	20
PC5	8	9
Total	79	72

Table 1.2 Random Forest variable ranking for maize and winter wheat. Rank 1 signifies the most important variable to determine yield. Values are determined by the number of climate index occurrences for each ranking for all climate divisions.

Climate Mode	Maize					Winter Wheat				
	Rank 1	Rank 2	Rank 3	Rank 4	Rank 5	Rank 1	Rank 2	Rank 3	Rank 4	Rank 5
AMO	111	63	37	23	6	74	56	32	32	28
NAO	6	13	33	50	138	37	25	48	52	60
ENSO	14	42	58	72	54	24	47	43	50	58
PDO	47	58	55	48	22	36	50	58	41	37
PNA	62	54	57	47	20	51	44	41	47	39

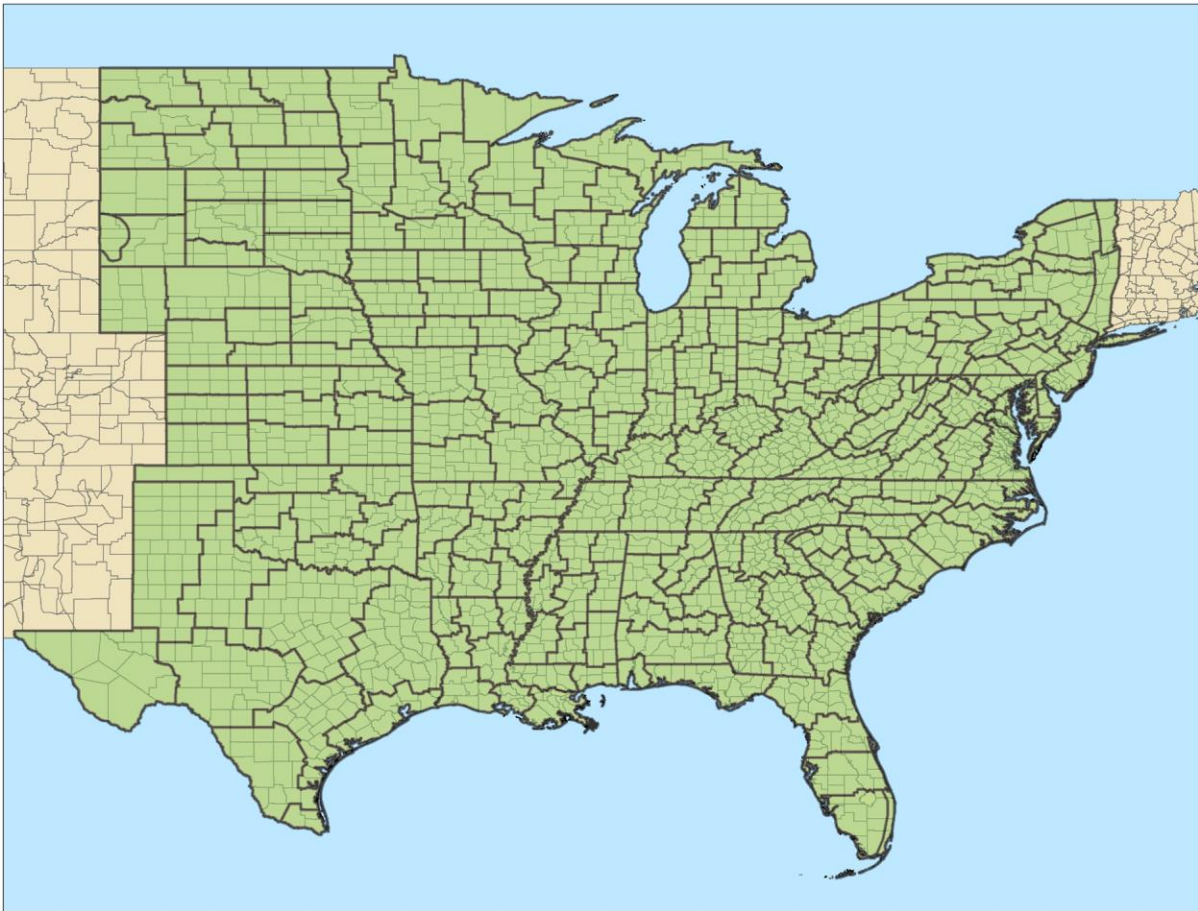


Figure 1.1 The study region is highlighted in green. Climate divisions in the study region are contoured in black, counties in gray.

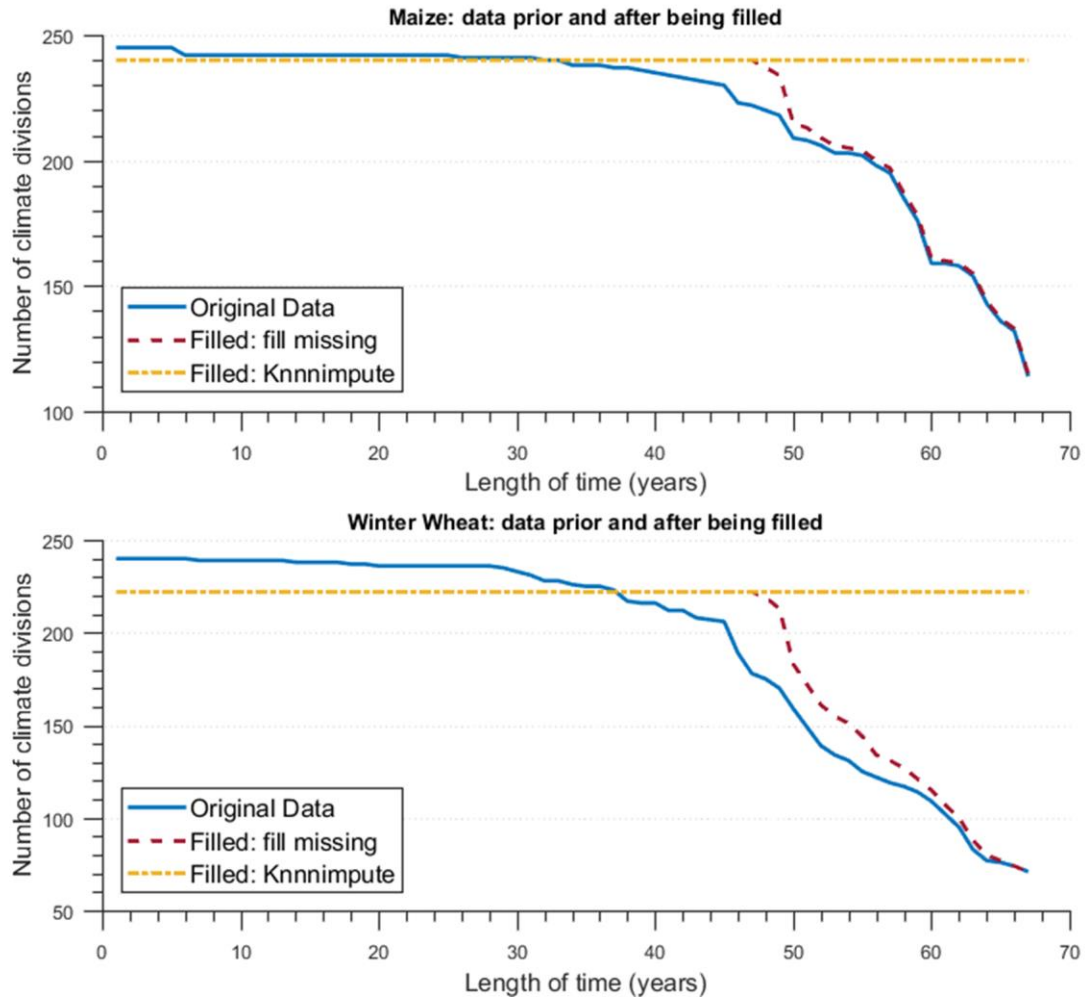


Figure 1.2. The number of climate divisions that have the specified years of data. The original data (blue line) was filled, if under the threshold, first using moving mean (red line) with a 10 year window. Second with KNN Imputation (yellow line), nearest neighbor. A five year moving average was applied and detrended. The number of climate divisions remaining for the maize data is 240 while winter wheat has 222.

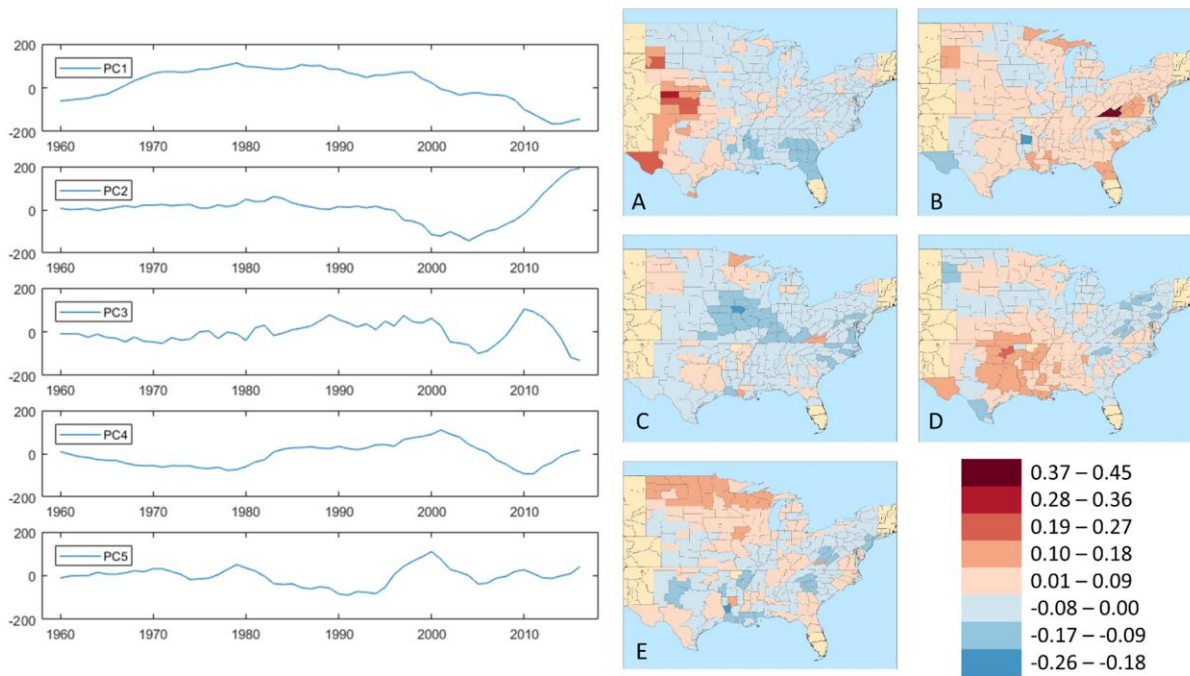


Figure 1.3 Patterns of spatial and temporal variability for maize yields, as revealed by the rotated principal component analysis (PCA). Spatial plot A is the loadings for the first principal component (PC1), B is for PC 2, C is for PC 3, D is for PC 4, and E is for PC 5.

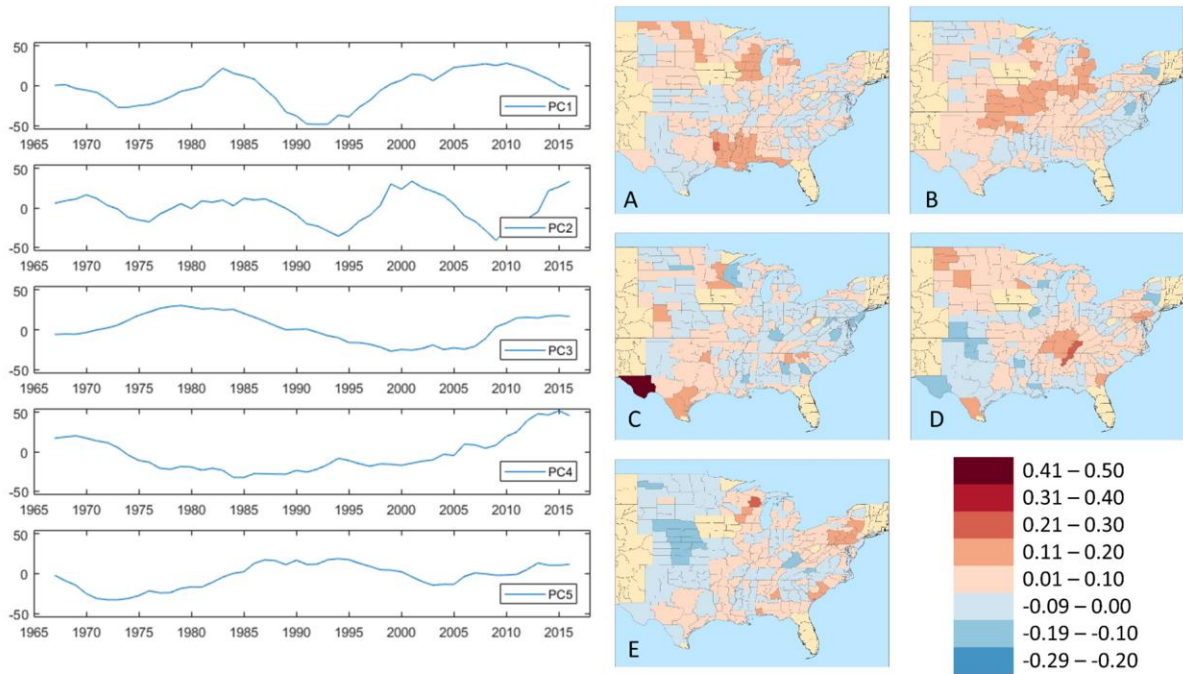


Figure 1.4 Same as in Figure 1.3, but for winter wheat.

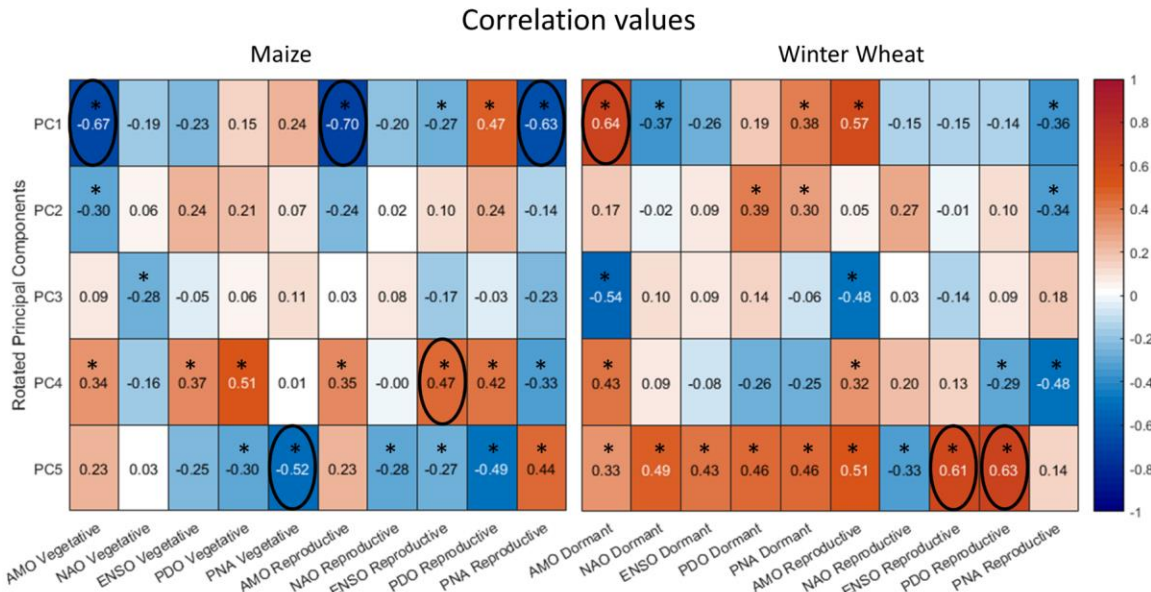


Figure 1.5 Correlation matrix of rotated principal components and the climate indices during the vegetative and reproductive growing periods for maize (Left Panel). Correlation matrix of rotated principal components and the climate indices during the dormant and reproductive growing periods for winter wheat (Right Panel). * Denotes significant values identified by *t*-test. Circled are significant values at the 95% level identified using a Monte Carlo approach.

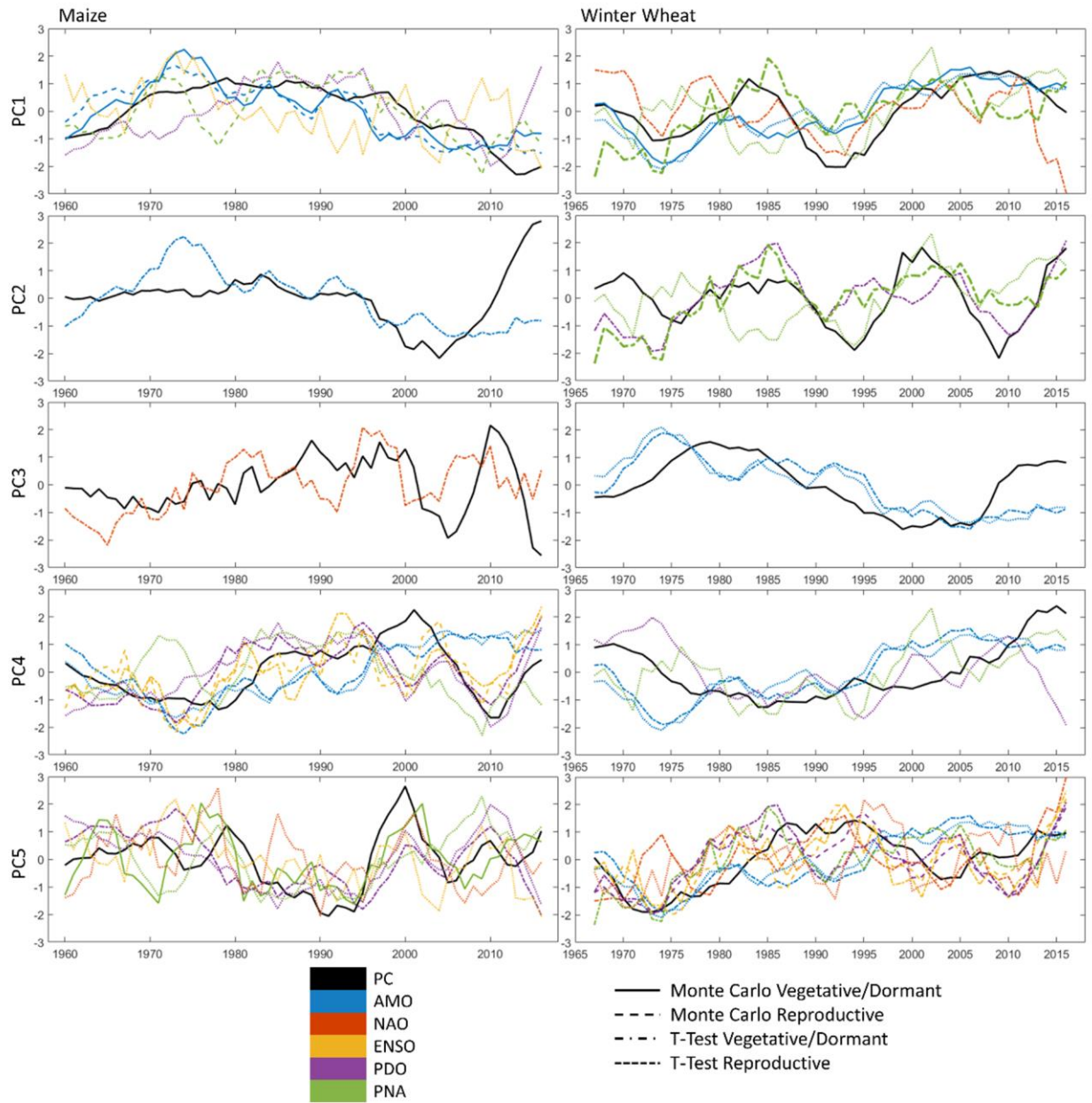


Figure 1.6 PC scores for maize (column 1) and winter wheat (column 2). Significant Monte Carlo (solid and dashed) and t-test (dash-dotted and dotted) results are plotted. Climate indices were significant for the Monte Carlo test were also significant for the t-test. PC scores are indicated by the thick black line, negative correlations have been multiplied by -1 for easier comparison.

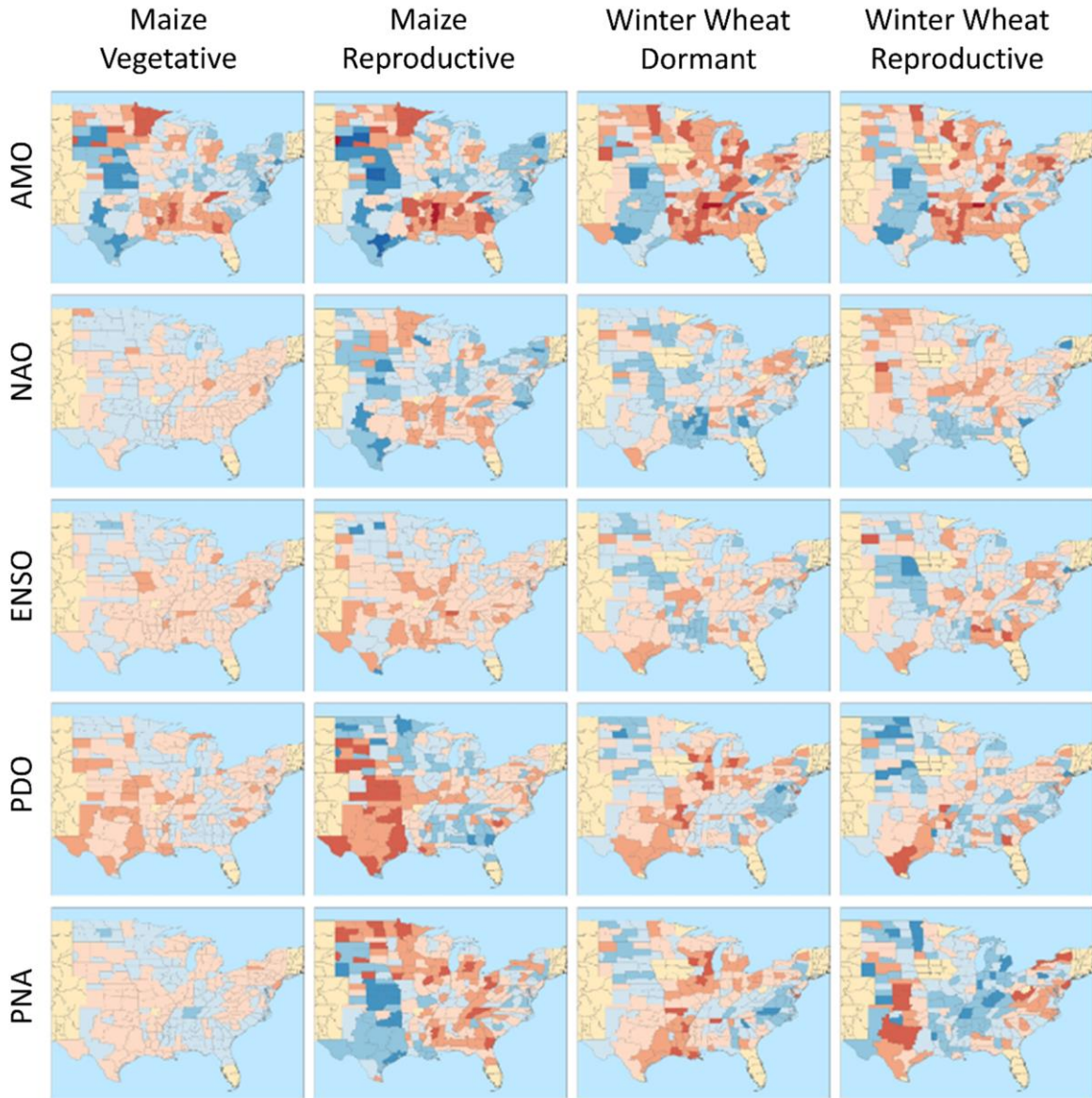
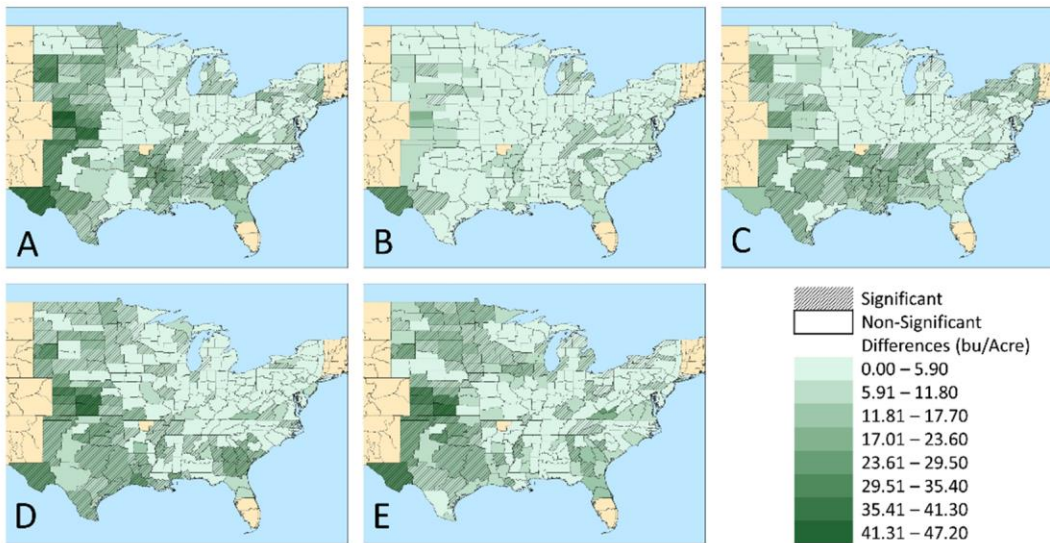


Figure 1.7 Correlation values between yield and climate indices. Dark blue values indicate stronger negative correlations and dark red values indicate climate division with strong positive correlations.

Maize



Winter Wheat

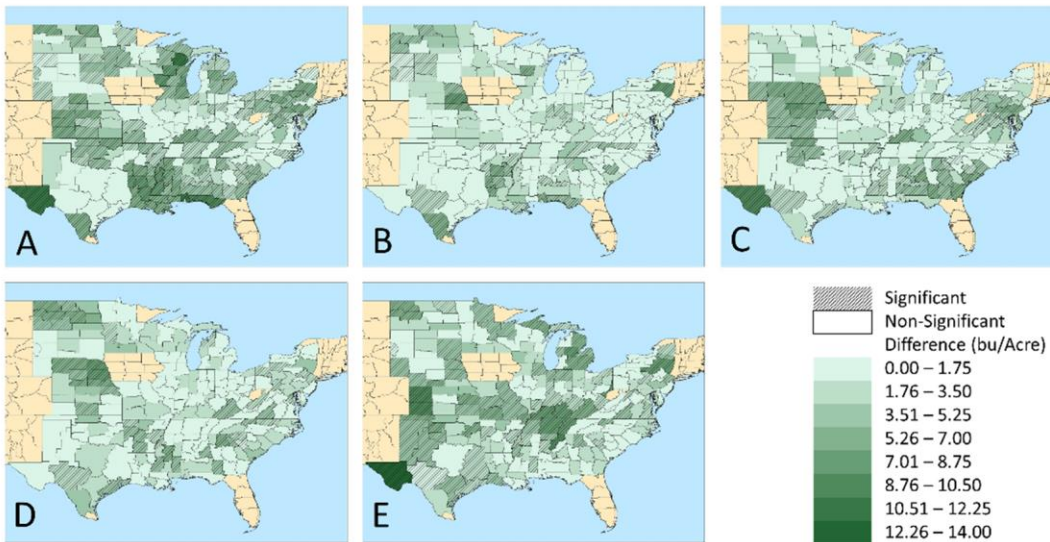


Figure 1.8 The differences between average yields during upper tercile and lower tercile of each climate index. A t-test was utilized to determine the significance at the 95% level, represented by the hatched regions. (A) AMO, (B) NAO, (C) PDO, (D) PNA, and (E) ENSO. A larger difference in yield anomalies is indicated by darker colors.

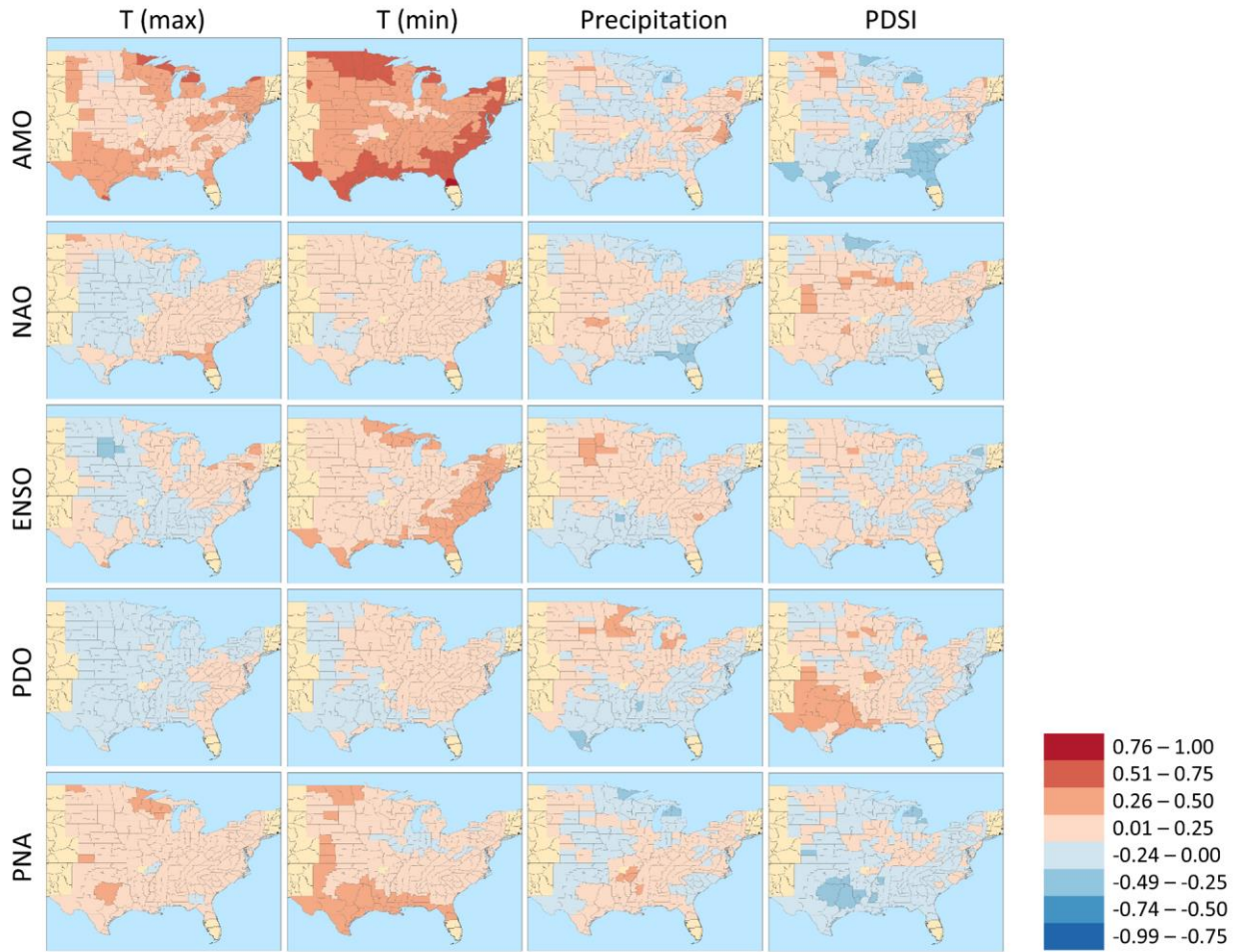


Figure 1. 9 The correlations between climate indices and surface climate variables during the reproductive period of maize.

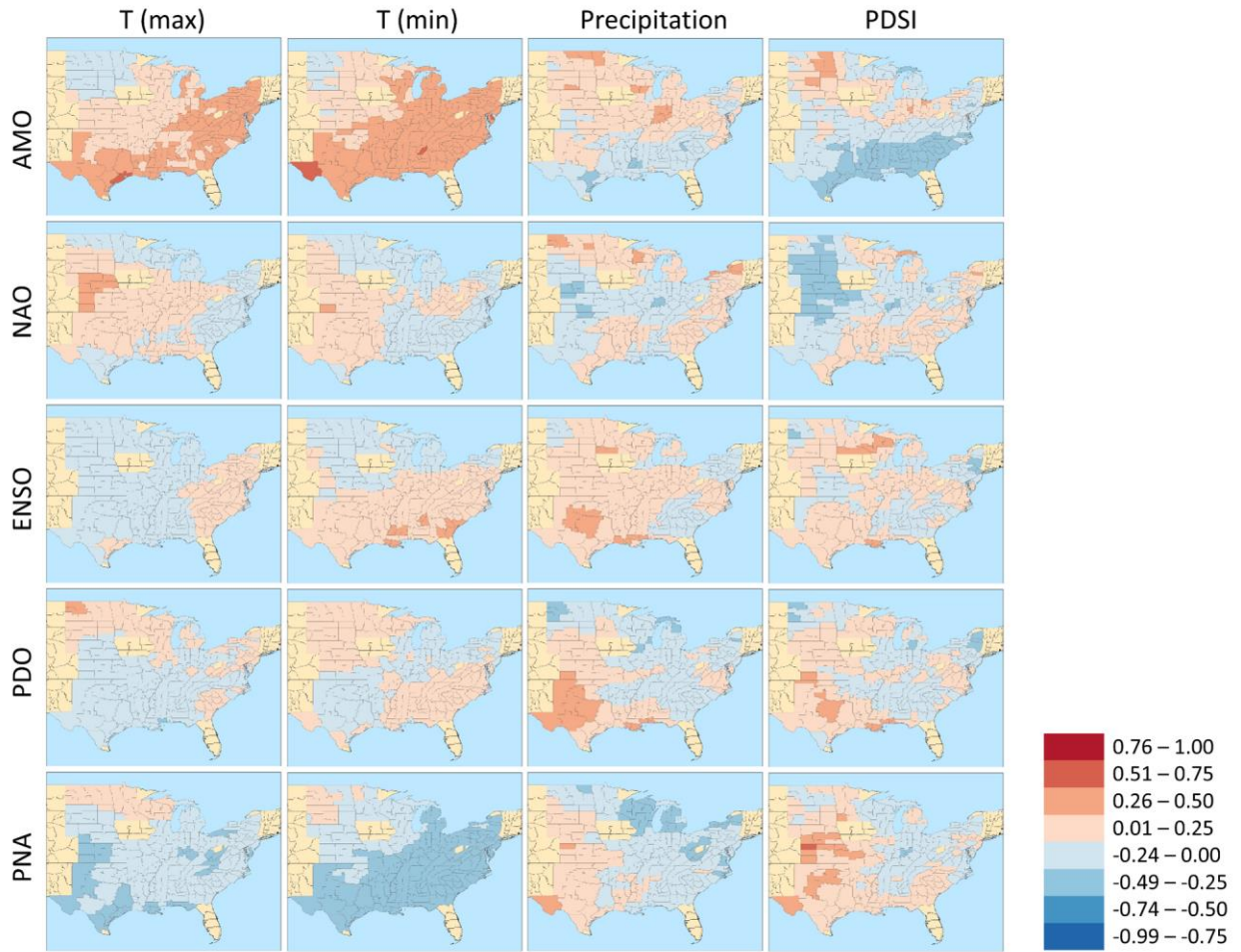


Figure 1.10 The correlations between climate indices and surface climate variables during the reproductive phase of winter wheat.

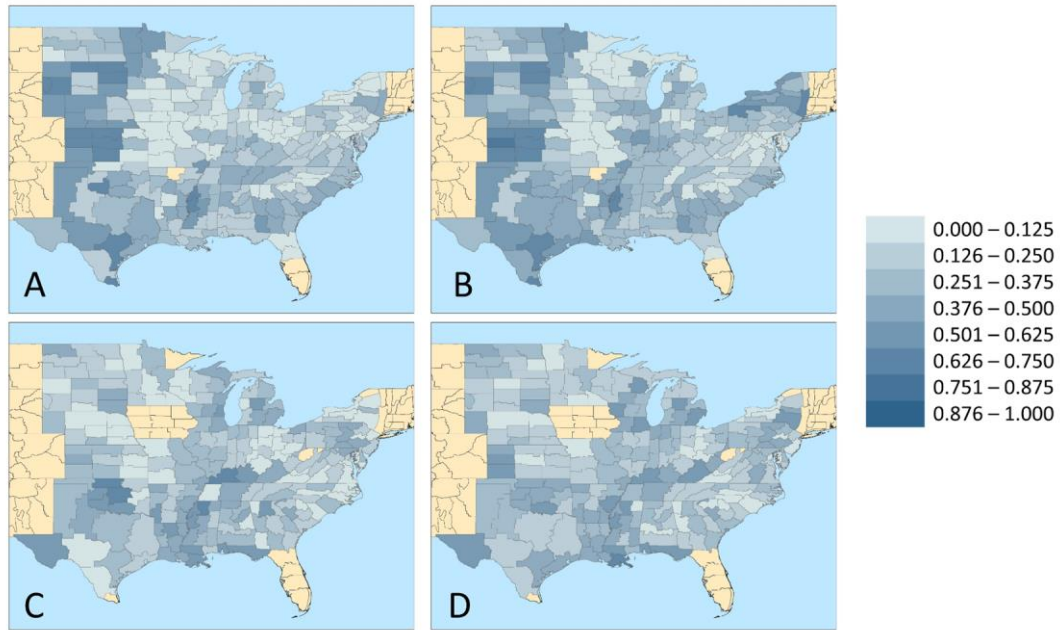


Figure 1.11 Adjusted R² of linear regression for (A) Vegetative and (B) Reproductive phase for maize and the (C) dormant and (D) reproductive phase for winter wheat.

Maize

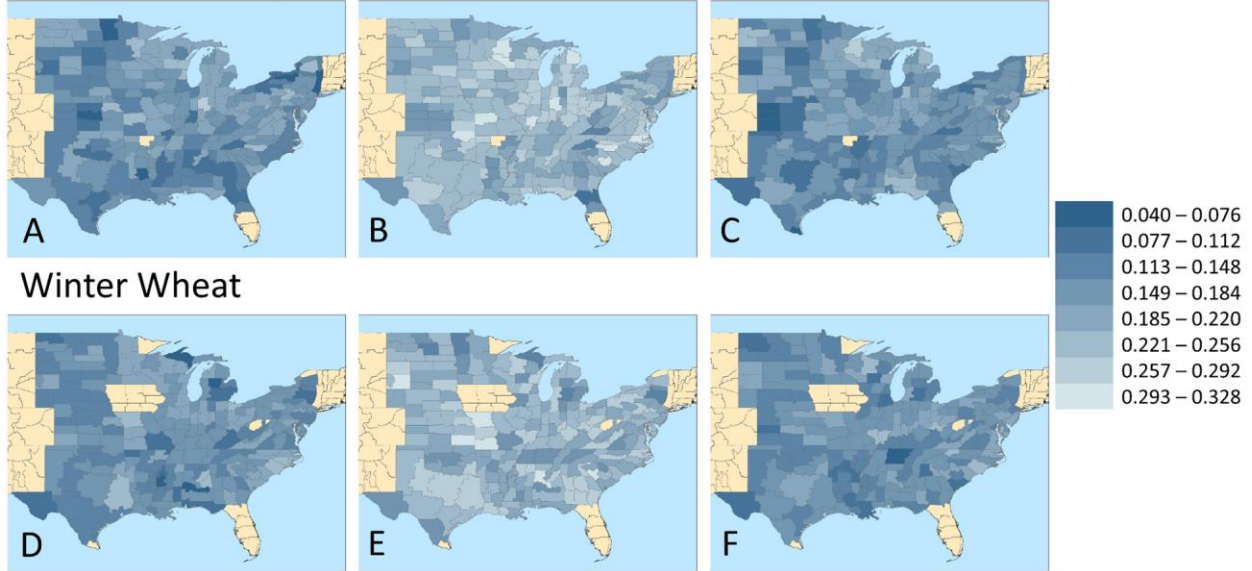


Figure 1.12 The spatial representation of the Brier Score for maize and winter wheat; high yields (A and D), average yields (B and E), and low yields (C and F). A Brier score value of 0 indicates a perfect forecast.

Chapter 2

Crop failure risks changes in the United States associated with large-scale climate oscillations

(This chapter has submitted for publication in Environmental Research Letters)

Abstract

Regions that produce a large supply of agriculture commodities can be susceptible to crop failure, thus causing concern for global food security. The United States, as one of the major agricultural producers in the world, is influenced by several large-scale climate circulations that contribute to climate variability: Atlantic Multidecadal Oscillation (AMO), North Atlantic Oscillation (NAO), El-Niño Southern Oscillation (ENSO), Pacific Decadal Oscillation (PDO) and Pacific-North American (PNA). Since local weather conditions are associated with these climate circulations through teleconnections, they are potentially causing changes of crop failure risks. The objective of this study is to assess climate-induced changes of annual crop failure risks for maize and winter wheat from 1960 to 2016, by analyzing the associations of large-scale climate circulations with the frequency of crop failure in the rainfed regions of the United States using a Bayesian approach. The result shows that a positive phase of AMO greatly increases the frequency of maize crop failure. Maize crop failure frequency increased when AMO and PDO are in positive and negative phases respectively, likely due to increased drought conditions. Crop failure for both maize and winter wheat increases when ENSO and PDO are out of phase. These results revealed the plausible drivers of long-term changes of U.S. crop failure risks and underscore the need for improving seasonal climate forecasting for sustainable agriculture.

1. Introduction

Agriculture systems in the modern era are becoming more interconnected, relying on high producing grain regions deemed breadbaskets. Just over 23% of the total world cropland produces the majority of the world's cereal crops (Janetos et al., 2017). Agriculturally developed regions are more likely to be at risk for reductions in yield and crop failure as they reduce their diversity in crops (Lesk et al., 2016). Among most vulnerable regions are mid-latitude countries, including China and the central United States (Teixeira et al., 2013).

Many environmental factors contribute to crop failure such as drought, pest, political turmoil or a combination of factors (Akresh et al., 2011; Gaupp et al., 2017; Goodwin, 2001; Lesk et al., 2016; Oerke, 2006; Sperling, 1999). Globally weather extremes can cause over a 30% reduction in yields and are expected to increase as agriculture systems become less diverse increasing vulnerability (Gbegbelegbe et al., 2014). Mendelsohn (2007) found that in the United States, 39% of the variance in crop failure is attributed to the combination of temperature, precipitation, and soils.

Globally, heat and drought events can be linked to crop failure. In Russia, combined extreme persistent heat and drought conditions caused wheat crop failure in 17% of planted cropland (Lau, Kim, Lau, & Kim, 2012; Wegren, 2011). Combined with society turmoil, wheat failures, and a ban on wheat exports caused bread, grain, and other commodities prices to rise despite government efforts to reduce panic. While Russia experienced one of their longest heat and drought events on record, Pakistan experienced record flooding, destroying crops creating a need for imports (FAO, IFAD, UNICEF, WFP, & WHO, 2018). Teleconnections and positive feedbacks allowed both events to persist and be amplified until the late summer of 2010 (Lau et al., 2012).

The history of crop failure in the United States has experienced several events since 1980, the most recent being the droughts of 1988 and 2012, and the flooding of 1993. A strong El Niño in the two years before 1988 promoted heat and drought conditions in the Midwest (Kovats et al., 2003; NOAA, 1988; Trenberth, Branstator, & Arkin, 1988). These conditions persisted into the 1988 crop season stunting crop growth during critical growing periods. A strong La Niña and unforgiving polar jet stream influenced the winter of 2011-2012, limiting winter precipitation in the plains (Mallya, Zhao, Song, Niyogi, & Govindaraju, 2013; Rippey, 2015). Lack of winter precipitation caused a quick depletion of soil moisture reserves in the growing season. The 1993 flooding event is attributed to persistent heavy rains in the Midwest, causing saturated soils and levee failures (Lott, 1993). The saturated soils caused a depletion in soil oxygen and promoted disease. All three events caused multi-billion dollar losses in agriculture and property damages. Crop failure ranged from around 20% to nearly 70% in regions around the Midwest (Kogan, 2002; NOAA, 1988; Rippey, 2015; Rosenzweig, Tubiello, Goldberg, Mills, & Bloomfield, 2002).

Globally, one-third of yield variability can be attributed to climate variability (Ray et al., 2015). Climate variability impact two-thirds of the global cropland, including high grain producing regions (Heino et al., 2018). A climate oscillation is a reoccurring large-scale ocean-atmospheric circulation that can cause climate variability. One such oscillation is the El Niño Southern Oscillation (ENSO) which has been the subject of many global and regional studies with its weather impacts influencing agriculture, health, and disease (Kovats et al., 2003; Vincenti-Gonzalez et al., 2018). Agriculturally, both positive and negative phases of ENSO cause a significant yield reductions in maize, soybeans, rice, and wheat globally. The El Niño phase is known to cause significant decreases in yield in Central America and the southeastern

United States (FAO et al., 2018; Martinez et al., 2009). The El Niño phase is known to cause significant decrease in yields by increasing drought conditions in Central America and cool, wet conditions in the Southeast United States.

Besides ENSO, other climate oscillations influence local and regional weather conditions which may also affect global agriculture. Atlantic Multidecadal Oscillation (AMO) is defined by 60-80 year oscillation of sea surface temperatures and originates in the North Atlantic Ocean (Delworth & Mann, 2000; Kerr, 2000). AMO causes changes in precipitation promoting drought in the United States and temperature changes in Brazil and China (Enfield et al., 2001; Knight et al., 2006; Li & Bates, 2007; McCabe et al., 2004). The North Atlantic Oscillation (NAO) also originates in the North Atlantic Ocean but is defined by pressure differences and a shorter oscillation period (Dahlman, 2009; J. W. Hurrell, 1995; Wang & You, 2004). NAO prominently influences the intensity of winter conditions in Asia, Europe, and the United States (Visbeck, 2002; Wang & You, 2004). Similar to ENSO, Pacific Decadal Oscillation (PDO) and Pacific North American (PNA) originate in the Pacific Ocean. Sea surface temperatures determine the PDO phase, while geopotential heights characterize PNA (Deser et al., 2016; Daniel J. Leathers et al., 1991; Mantua & Hare, 2002). PDO has similar but weaker spatial patterns compared to ENSO. It results in less precipitation in the Ohio and Tennessee River valleys and more precipitation along with the Southeast coastal states (Di Liberto, 2016). Similar to NAO, PDO influences winter weather in North America (Asong et al., 2018; Daniel J. Leathers et al., 1991). Influences in agriculture production have also been linked to these climate oscillations regionally and globally. AMO has been identified as a major factor associated with dominant spatial and temporal variations of maize and winter wheat yields in the United States (Schillerberg, Tian, & Miao, 2019). European agriculture experiences a decrease in wheat and varied spatial yield

response from maize under negative NAO conditions in the United States and shows a small increase in the average of wheat and maize yields (Kim & McCarl, 2005). PDO and ENSO interactions promote yield changes in the Midwest United States (Henson et al., 2017). Maize yields in the southeast United States are affected by PNA (Martinez et al., 2009). However, to the best of our knowledge, no study has yet been conducted to quantify the risks of crop failure associated with climate oscillations, in spite of its potential importance for informing food accessibility risk management, agricultural trading, and food security policy and decision-making.

Prior research on crop failure has focused on the impact of seasonal weather conditions, extreme climate, and pests and diseases (e.g. Deutsch et al., 2018; Tigchelaar et al., 2018; Zampieri et al., 2017). Few studies have shown the connections between crop failure events and how climate variability, through climate oscillations may increase the probability of crop failure. This study aims to use Bayesian analysis to assess the changes of crop failure risks in the rainfed regions of the United States, a breadbasket of the world, associated with five influential climate oscillations, their phases, and combinations of oscillations. Following the analysis, there is a discussion of probable causes leading to crop failure, resulting from known impacts of climate oscillations. The knowledge and information gained from this study will be useful for informing food security management, agribusiness, and climate risk management in agriculture.

2. Data and Methods

2.1 Study Area

The area of study is the eastern rain-fed regions (100°W Meridian) of the United States. Nearly 90% of the region is rain-fed, however extensive irrigation exist in portions of central Nebraska, western Kansas, the panhandle of Texas, eastern Arkansas and southwest Georgia

(NASS, 2014a, 2014b). Since irrigation can counteract the climate impacts, climate variability plays a less important role over these irrigated regions. The analysis is conducted at the climate division level. In the United States, states are separated into climate divisions composed of several smaller counties. Climate divisions, often used for climatic purposes experience homogeneous weather conditions (Karl & Riebsame, 1984). Therefore, allowing spatial variation, on a smaller scale as opposed to a state or national spatial scale.

2.2 Yield data and climate indices

Annual county-level crop yield and production data were retrieved for maize and winter wheat from 1960 to 2016 from the National Agricultural Statistic Service (NASS) of the United States Department of Agriculture (USDA) (via <https://quickstats.nass.usda.gov/>). These crops are considered as the most important summer and winter crops in the United States. Since each climate division usually covers multiple counties, maize and winter wheat yields for each climate division were calculated using weighted averages of county-level yields where county-level yield productions were used as weights. After the weighted average, the crop yield over each climate division is homogeneous. Preprocessing and quality control are conducted to ensure the spatial and temporal completeness of climate division yield data. First, the data quality is checked; climate divisions having less than 70% of their data are removed. Next, missing yield data were filled through two steps. The first step is to fill the data gap using a moving median with a window of 10 years. The second step fill the rest gaps using the K-Nearest Neighbors (KNN) Imputation, which has been widely used in many biological and spatial studies to fill missing data (e.g., Tian et al., 2017; Wilson et al., 2004). After preprocessing, the yield data was detrended to minimize the combined effects of changes in agro-management practices, technology, socio-economic factors, and climatic changes. The preprocessing methods resulted in complete

datasets of 240 climate divisions for maize from 1960 to 2016; and 222 climate divisions for winter wheat from 1967 to 2016.

Monthly climate indices data for quantifying climate oscillations, AMO, NAO, ENSO, PDO, and PNA, are obtained from different sources, including Earth System Research Laboratory at National Oceanic and Atmospheric Administration (NOAA), National Center for Atmospheric Research (NCAR), the Joint Institute for the Study of Atmosphere and Ocean at the University of Washington, and NOAA Climate Prediction Center. Climate indices data are processed by taking an average of the three months prior to harvest, which are July, August, September for maize and April, May, June for winter wheat (Berglund et al., 2013; Hall & Nleya, 2012; Iizumi et al., 2014; Nleya, 2012; Sacks et al., 2010). These periods cover the reproductive stage (Ceglar et al., 2017; Mourtziniss et al., 2016), a time when crops are more sensitive to their climate environments.

2.3 Bayesian Analysis

For this study, a crop failure occurs when the yield falls under the lower quartile of all the yields of a climate division. Defining crop failure as the lower quartile allows the capture of regional events that may have decreased yield production like drought. However, this method may not capture total crop failure due to such events like hail, or instances where producers changed intended crop use and not reported yield reductions to NASS (Nleya, 2012). We analyze the crop failure risks use a similar Bayesian approach employed by Kam et al. (2014). Each crop failure for a climate division is treated as a sample of a Bernoulli process, and each crop failure occurrence X follows a Bernoulli trial with crop failure occurrence equals 1 and non-crop failure occurrence equals 0. Over 1960 to 2016, there are 14 and 13 crop failures for maize and winter

wheat respectfully; this is used to calculate the expected frequency of 0.25 for both crops agreeing with the chosen lower quartile threshold.

The Bayesian analysis approach allows the use of the Bernoulli process to compute the posterior distribution of crop failure. Thus, the prior distribution is a conjugate of the likelihood distribution, given that the prior and the posterior distributions belong to the same family (Benjamin & Cornell, 1970; Casella & Berger, 2002). The posterior distribution of crop failure is computed as the prior distribution multiplied by the likelihood function.

$$\text{Posterior} \propto \text{Prior} \times \text{Likelihood}$$

The prior distribution is treated as an uninformed prior, which is equivalent to the beta distribution where alpha and beta are equal to 1 (Wilks, 2011). The posterior distribution can be computed with a new alpha ($s+1$) and beta ($n-s+1$) parameters (Benjamin & Cornell, 1970). Where s is the number of crop failure occurrences in n , the number of years, these are considered sufficient Bernoulli-process sample statistics (Benjamin & Cornell, 1970). Therefore the final equation to calculate the posterior distribution as a function of p , crop failure frequency is:

$$f(p; s, n - s) = \frac{1}{B(s + 1, n - s + 1)} p^s (1 - p)^{n-s}$$

Where $B(s+1, n-s+1)$ is the beta function.

In order to examine the impact of climate oscillations on crop failure occurrence, conditional posterior distributions of crop failure are computed based on a subset of the crop yield data given the phase of climate index: $\Pr\{p|X, Y\}$, where Y is the phase of climate index. The conditional posterior distributions are computed for each climate division and compared with the posterior distribution derived using the full crop yield data. An increase in crop failure frequency occurs when the expected value of the conditional posterior distribution for crop failure is greater than that of the original posterior distribution $\Pr\{p>0.25|X, Y\}$. Significant

increase in crop failure frequency occurs when the expected value of the conditional posterior distribution meets or exceeds the 90th percentile of the original posterior distribution.

3. Results and Discussion

3.1 Time series of crop failure

The percentage of climate divisions that experienced annual crop failure is calculated for maize and winter wheat and shown as a time series in Figure 2.1. The time series allows for further examining the progression of crop failure events and how they coincide with historical records in the rainfed United States.

On average, there are 25% climate divisions experiencing crop failure over 1960-2016. Maize shows an increase in crop failure events from 1960 to 1986. While the volatile crop failure from 1987 to 2013 results in no trend change, there is a decrease trend in crop failure percentages of 2014 to 2016. Years with a high percentage of climate divisions experiencing crop failure are 1988, 1993, 2002, 2011 and 2012, when there are widespread heat, drought, and flooding throughout the growing seasons over these years. For example, in 1988, when there was a devastating drought in North America (Opie, 1992), nearly 70% of maize producing climate divisions experienced crop yields in the lower quartile of their reported yields (Figure 2.1).

Winter wheat also shows a slight increase in crop failure from 1967 to 1993. After this period, the crop failure percentage has no apparent trend. Like maize, winter wheat experienced an average of 26% of the climate divisions experiencing crop failure from 1967 to 2016. The largest increase in crop failure percentage occurred in 1991, where 61% of climate divisions are affected. Historical records show that this event was likely due to heavy spring rains which, promoted the growth of diseases (Merry, 1991; United Press International, 1991). Other years where nearly 50% of climate divisions experienced crop failure is 1993 and 1996 due to flooding

and drought conditions, respectively (Bureau of Labor Statistics & U.S. Department of Labor, 1998; Lott, 1993).

3.2 The impact of individual climate oscillation on maize crop failure frequencies

The difference in the number of climate divisions experiencing significant increases in crop failure frequencies under opposing oscillation phases is the largest between AMO phases. As noted previously, a large extent of spatial area under positive AMO conditions experience an increase in crop failure frequency, with 70 climate divisions experiencing significant increases in frequency. In contrast, under negative AMO conditions, the eastern United States largely experiences a decrease in frequency with only six climate divisions experiencing a significant increase in frequency. The drastic changes in frequency is likely a result of the association between AMO and drought in the United States, as noted by Enfield et al. (2001), Kam et al. (2014), and McCabe et al. (2004). Drought occurrences influenced by AMO are likely to extend multiple years due to AMO's long oscillation period. These long-lasting droughts may deplete soil moisture reserves, affect all growth stages, and have the potential to reduce yield more than 60% (Çakir, 2004; H. Song, Li, Zhou, Xu, & Zhou, 2018). Drought during the reproductive stage can affect yield, dry matter weight, and leaf area (Çakir, 2004; Denmead & Shaw, 1960; Saini & Westgate, 1999).

A negative PNA significantly increases the crop failure frequency in 53 climate divisions, making it the second largest influencer of maize failure frequency (Table 2.1). While positive AMO excludes the northern Great Plains, this is an area where negative PNA increase crop failure frequency. However, negative PNA decreases crop failure frequency in western Nebraska to Texas and the Carolinas. It is worth noting that PNA during June and July, a likely transition period, has little impact on climate conditions (Daniel J. Leathers et al., 1991). Therefore, a

negative PNA would be influencing late grain fill, but a positive PNA, commonly associated with drought, is influencing the vegetative period (Climate Prediction Center Internet Team, 2012; Daniel J. Leathers et al., 1991). Drought conditions experienced during the vegetative stage have lasting negative impacts contributing to a reduction in yield (Çakir, 2004; Mangani et al., 2018).

Positive NAO and negative ENSO result in 35 and 30 climate divisions respectively experiencing significant increases in crop failure frequency. For positive NAO regions experience an increase in frequency is the northern Midwest and eastern Texas to western Mississippi, similar to Heino et al. (2018), this area is one of the most sensitive regions to NAO phase. However, Heino et al. (2018) found an increase in 12 simulated crops production under a positive NAO phase. A negative NAO phase results in 17 significantly negatively impacted climate divisions, with vast portions experiencing no change in crop failure frequency. The lack of negative impacts on yields agrees with the slight yield increase under negative NAO phase, as found by Kim & McCarl (2005).

The results also indicate that negative ENSO conditions cause an increase in crop failure in the Ohio Valley region, while a positive phase ENSO results in a decrease in crop failure. Spatial patterns of crop failure frequencies are consistent with yield changes due to ENSO noted by Henson et al. (2017) and Iizumi et al. (2014). A negative ENSO phase results in more precipitation in the eastern Midwest, when combined with warmer temperatures may promote the growth of diseases and other pest, negatively influencing crop yields. Excess precipitation before planting can delay planting and prevent field maintenance during the vegetative period. Both are examples of how crop yields can be reduced prior to the reproductive period because of excess moisture (Baum et al., 2019).

The phases of PDO result in a similar amount of climate divisions experiencing significant increases in crop failure frequency; a positive PDO results in slightly more climate divisions experiencing a significant increase in crop failure than a negative phase (Table 2.1). Similar to previous oscillations, there is a distinct spatial pattern in crop failure frequencies under different phases. For a positive PDO, an increase in crop failure frequency stretches from the upper Midwest to the Southeast with the decrease in crop failure primarily being in the south and plains region. A more pronounced pattern is true for a negative PDO. Spatial patterns of the crop failure under both PDO regimes agree with the spatial distribution of drought frequency increases found by Kam et al. (2014).

3.3 The impact of individual climate oscillation on winter wheat crop failure frequencies

Unlike maize, winter wheat has a smaller portion of climate divisions experiencing a significant increase in crop failure, 29% vs. 16%, respectively (Table 2.1). The number of climate divisions experiencing significant crop failure varies from the highest at 16% (37 climate division) under positive NAO conditions to 0% under negative NAO conditions. The changes of NAO phases result in the largest difference in the number of climate divisions (37) experiencing significant increase of winter wheat failure frequencies. On average, the difference in the number of climate divisions experiencing significant increase of winter wheat failure frequency under positive and negative climate oscillation phases is equal to 12. This finding suggests that the winter wheat crop failure risk is more sensitive to the changes of NAO phases than the other climate indices. Regions that experience a significant increase in crop failure varies by mode phases (Figure 2.2, right panel). However, two regions consistently experience a significant increase in crop failure for several modes. The first region, extending from the Ohio River valley to Louisiana experiences crop failure under negative AMO, positive NAO, positive ENSO, and

negative PDO. The second region, western Texas, experiences an increase in crop failure when AMO is positive, NAO is positive, ENSO is negative, and PDO is negative.

Positive NAO results in two major areas of significant increase in crop failure, the Ohio River Valley near Indiana into Kentucky and western Texas through western Nebraska. Under positive NAO, the aforementioned areas see a decrease in frequency with the majority of the study area experiencing no change or non-significant increases in failure frequency. This finding is consistent with Kim & McCarl (2005), who previously noted that overall, there is a net increase in wheat yields under negative NAO conditions. Reasons for the increase in crop failure frequency under a positive NAO may be due to the warmer temperatures and decreased precipitation. The warmer winters may cause the winter wheat to come out of dormancy earlier increasing water demand, and thus resulting in increased susceptibility to spring frost and drought decreasing the quantity and quality of winter wheat yields (Nleya, 2012; Olgun et al., 2008; Trnka et al., 2014). In contrast, negative NAO conditions result in cooler, wetter conditions, which with proper hardening in the fall, the snow may act to insulate the wheat from frigid conditions and provide more moisture in the reproductive period.

A negative AMO resulted in the next highest number of significant climate divisions (33) experiencing crop failure (Table 2.1). Pennsylvania through the Ohio River Valley to Louisiana and Mississippi experience significant increases in crop failure frequency. The region of increased crop failure continues into the Midwest and eastern Kansas. North Dakota, Minnesota, far western Texas and portions of the Carolinas are the only regions that see a decrease in crop failure frequency during the negative AMO and an increase in failure frequency during the positive AMO. Negative AMO is associated with increases in precipitation, which may cause flooding (Enfield et al., 2001; Jeffrey C. Rogers & Coleman, 2003). Exposed lengths of time to

flooding or ponding water causes decreases in wheat yields as the plant diverts energy to the roots for oxygen (Olgun et al., 2008). The Dakotas and Minnesota may see a decrease in crop failure, because of slight a decrease in temperatures and increase in precipitation, while in positive phases the lack of precipitation results in increased vulnerability and drought conditions later in the reproductive period.

Positive ENSO conditions induce a significant increase in winter wheat failure in the southeast (Figure 2.2). This increase is likely due to cooler, wet conditions that can promote frost kill and growth of pest, both of which can significantly reduce winter wheat yields. This decrease in yields is consistent with the findings of Martinez et al. (2009). Ohio and northern Illinois and Indiana experience a significant increase in winter wheat failure during negative ENSO events. Likely due to wet conditions promoting flooding and pest similar to the southeast.

Positive PNA results in large portions from Georgia to North Dakota, experiencing non-significant increases in crop failure (Figure 2.2). Significant increases are present in northern Indiana and the eastern regions of the Dakotas, Kansas, and Oklahoma. Cold air from Canada may be promoting wheat failure due to cold outbreaks (Daniel J. Leathers et al., 1991). During negative PNA events, western Kansas, Nebraska, and portions of the east coast undergo increased frequencies of crop failure, likely due to colder damp conditions promoting the growth of fungus diseases (Cook, 2001; Cunfer, 2000) and flooding.

Positive and negative PDO result in a similar amount of climate divisions experiencing significant increases in crop failure (Table 2.1). The area of climate divisions experiencing increases in crop failure frequency is contrasting as noted with other oscillations. Positive PDO causes increases of crop failure frequency in the Great Plains and Southeast. While negative PDO increases crop failure in western Texas and Louisiana to Wisconsin. As expected, PDO and

ENSO of simultaneous phases have similar impact on spatial distributions of crop failure frequencies (Figure 2.2).

3.4 The combinations of climate oscillations impact on crop failure frequencies

Climate oscillations are known to interact with each other intensifying or weakening their impacts. McCabe et al. (2004) found the combination of AMO and PDO explained spatial and temporal variations in drought in the United States. ENSO and PDO are another climate oscillation combination that is of concern. This concern arises from similar spatial impacts under agreeing phases (Hu & Huang, 2009; Mantua et al., 1997), which means when phase sign agrees, there is a more substantial impact than when phases are in disagreement. The same Bayesian analysis method is performed to construct conditional posterior distributions with the likelihood function dependent on combinations of climate oscillations phases as well as the occurrences of crop failures.

3.4a. The combinations of AMO and PDO impact on crop failure frequencies

The number of climate divisions experiencing significant increases in crop failure frequencies varies widely among different AMO and PDO phase combinations (Table 2.2). When experiencing a positive AMO and negative PDO, there are largest number of climate divisions experiencing a significant increase in maize crop failure frequencies. Regions experiencing a decrease in crop failure are in the northern Great Plains and Arkansas (Figure 2.3). Conversely, simultaneous negative AMO and PDO have the least number of climate divisions experiencing significant increases in crop failure frequency. The main regions experiencing increased crop failure frequency are centered in Arkansas extending into western Oklahoma. The spatial patterns of the impact on crop failure frequencies in Figure 2.3 are consistent with the findings of the impact on drought in McCabe et al. (2004). AMO and PDO

combination impacts are concerning, because of their long oscillations, which means favorable crop failure conditions could persist for several years reducing global maize stores.

Compared to maize, no phase combination of AMO and PDO drastically increases the number of winter wheat climate divisions experiencing significant increases in crop failure frequency. The percentage of climate divisions experiencing significant crop failure frequency increases varies from 11% to 25% (Table 2.2). A positive AMO and negative PDO combination result in the largest contrast in space between significant increases and decreases in crop failure frequencies (Figure 2.3). The Southeast has the smallest crop failure frequency, while western Texas through Nebraska has the highest increases. Combinations of negative AMO and negative or positive PDO prompt more significant increases in crop failure compared to any of the individual oscillation. A similar spatial pattern is present in both negative AMO and negative or positive PDO combination, with the northeast to Texas showing increased crop failure frequency, when compared to the impact of individual AMO during negative phase. The combination of negative AMO and negative PDO result in the largest number of climate divisions experiencing a significant increase in crop failure frequency; this impacted region includes climate divisions over Texas, Louisiana into the Ohio River Valley and coastal areas.

3.4b. The combinations of ENSO and PDO impact on crop failure frequencies

Looking at an in-phase ENSO and PDO, the combination of the negative ENSO and negative PDO results in the largest amount of climate divisions experiencing significant crop failure (Table 2.3). Under these conditions, the southwestern Plains and the Carolinas experience a significant increase in crop failure frequency. This also coincides with regions that receive less precipitation when ENSO and PDO are negative (Di Liberto, 2016). When a positive ENSO and PDO are in phase, a similar opposite pattern occurs, aligning impacts and increased crop failure

frequency. When ENSO and PDO are out of phase, the largest number of climate divisions experiencing an increase in crop failure frequencies are presented (Table 2.3 and Figure 2.4). This increase may be a result of interactions between ENSO and PDO dampening their impacts, allowing other climate oscillation's impacts to have more of an impact. In particular, when ENSO and PDO are out of phase, their spatial patterns are similar to the spatial patterns of crop failure frequencies under PNA phases in Figure 2.2.

Similar to maize, winter wheat also experiences the largest number of climate divisions with significant increases in crop failure when ENSO and PDO are out of phase (Figure 2.4, Table 2.3). However, unlike maize, there does not appear to be a distinct oscillation impact pattern that aligns with an individual climate oscillation (Figure 2.2). When ENSO and PDO are in-phase, there are similarities to individual oscillations of ENSO and PDO crop failure frequencies. For example, increased crop failure frequency in southern Ohio River Valley and upper Midwest Plains region during positive in-phase ENSO and PDO aligns with the increases present respectively in positive ENSO or PDO in Figure 2.2.

4. Conclusions

The lowest quartile of crop yields was considered as crop failure and treated as trials in a Bernoulli process. Treating the crop failure as Bernoulli processes allowed for a Bayesian approach to be taken for analyzing crop failure frequency under each climate index's phase. The analysis shows that a positive AMO increases crop failure frequency for maize significantly in 29% of the climate divisions, likely due to drought conditions present throughout the growing and reproductive period. In contrast, a negative AMO results in a significant increase in crop failure of maize in six climate divisions. Negative PNA is also notable in increasing the crop failure frequency of maize in many climate divisions and significantly increasing in 53 climate

divisions. Winter wheat experiences a lower number of climate divisions with significant increases in crop failure frequencies, likely due to higher levels of soil moisture from the winter months persisting into the reproductive period of spring and early summer. In positive NAO conditions, 37 climate divisions experience significant increases in crop failure frequency, the largest among individual phases of climate oscillations. During negative NAO phases, climate divisions experience non-significant increases in crop failures.

Phase combinations of AMO and PDO as well as ENSO and PDO were also analyzed to determine their impacts on crop failure frequency. Climate divisions experiencing significant maize crop failure frequency increased to 131 when a positive AMO negative PDO occurs. The largest decrease in crop failure frequency occurs when a negative AMO and positive PDO occur. Winter wheat crop failure increased when a negative AMO occurs with a negative PDO combination experiencing slightly more than a negative AMO positive PDO combination. The combination of ENSO and PDO showed that when the indices are out of phase, the magnitudes of the failure frequencies increase. A positive ENSO and negative PDO resulted in the highest number of climate divisions (135) experiencing a significant increase in their crop failure frequency for winter wheat.

Knowledge of increases and decreases in crop failure frequency due to climate indices have the potential to improve seasonal crop yield forecasting, because of the cyclic nature and predictability of climate indices. Advances in seasonal climate forecasting would allow for a better prediction of climate oscillations, leading to an improvement in agribusinesses handling of operation and crop loss costs, seasonal climate risks, and mitigation practices to decrease vulnerability. Programs focused on food security, (e.g. FEWS NET) would better be able to

predict changes in global grain stores and price fluctuations that may be a result of crop failure in the United States.

Table 2. 1 The number of climate divisions that experience a significant increase in crop failure at the 90th percentile for maize and winter wheat under different phases of climate indices.

Crop	Climate Index	Phase	Number of Climate Divisions
Maize	AMO	+	70
	AMO	-	6
	NAO	+	35
	NAO	-	17
	ENSO	+	9
	ENSO	-	30
	PDO	+	23
	PDO	-	15
	PNA	+	14
	PNA	-	53
	Winter Wheat	AMO	+
AMO		-	33
NAO		+	37
NAO		-	0
ENSO		+	29
ENSO		-	15
PDO		+	16
PDO		-	21
PNA		+	25
PNA		-	12

Table 2.2 The number of climate divisions that experience a significant increase in crop failure at the 90th percentile for maize and winter wheat under different combinations of AMO and PDO phases.

Crop	Phase Combination		Number of Climate Divisions
Maize	AMO +	PDO +	62
	AMO +	PDO -	131
	AMO -	PDO +	30
	AMO -	PDO -	11
Winter Wheat	AMO +	PDO +	34
	AMO +	PDO -	25
	AMO -	PDO +	49
	AMO -	PDO -	55

Table 1.3 The number of climate divisions that experience a significant increase in crop failure at the 90th percentile for maize and winter wheat, while experiencing the indicated combination climate oscillation phases of ENSO and PDO.

Crop	Phase Combination		Number of Climate Divisions
Maize	ENSO +	PDO +	17
	ENSO +	PDO -	33
	ENSO -	PDO +	131
	ENSO -	PDO -	48
Winter Wheat	ENSO +	PDO +	36
	ENSO +	PDO -	135
	ENSO -	PDO +	99
	ENSO -	PDO -	9

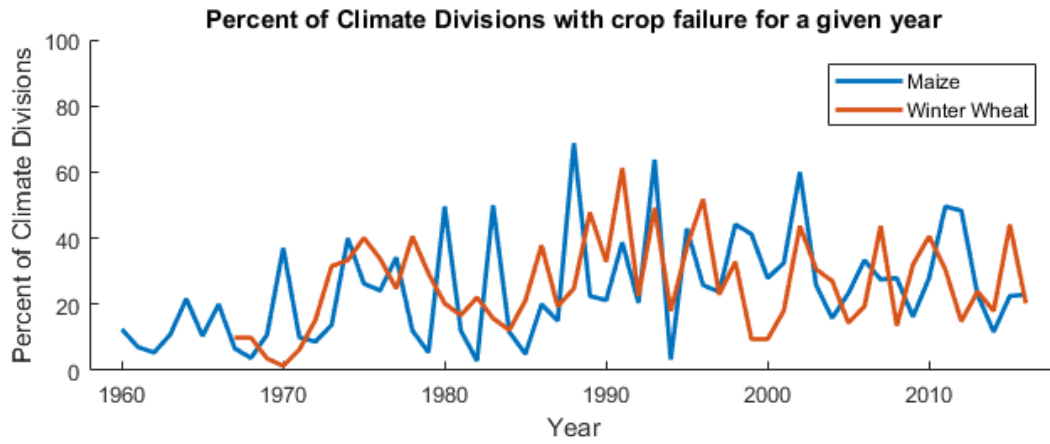


Figure 2.1 Time series displaying the percent of climate divisions experiencing crop failure for maize and winter wheat in the eastern United States.

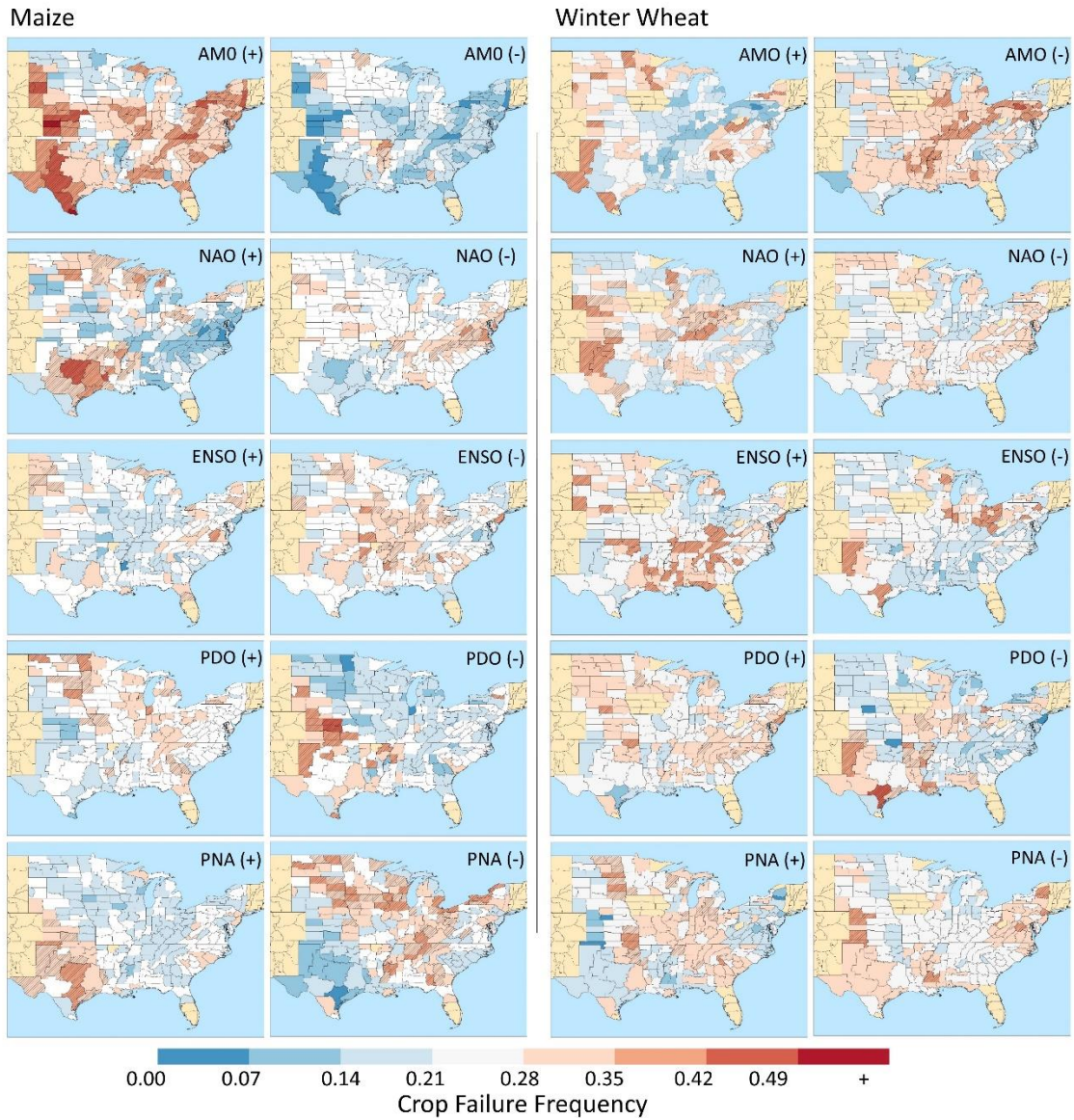


Figure 2.2 Annual crop failure frequency of maize (left) and winter wheat (right) during each phase of climate indices. Climate divisions with blue coloring indicate a decrease in crop failure relative to the posterior distribution, while red divisions indicate an increase. Hashed climate divisions indicate significant increase in crop failure frequency at the 90th percentile.

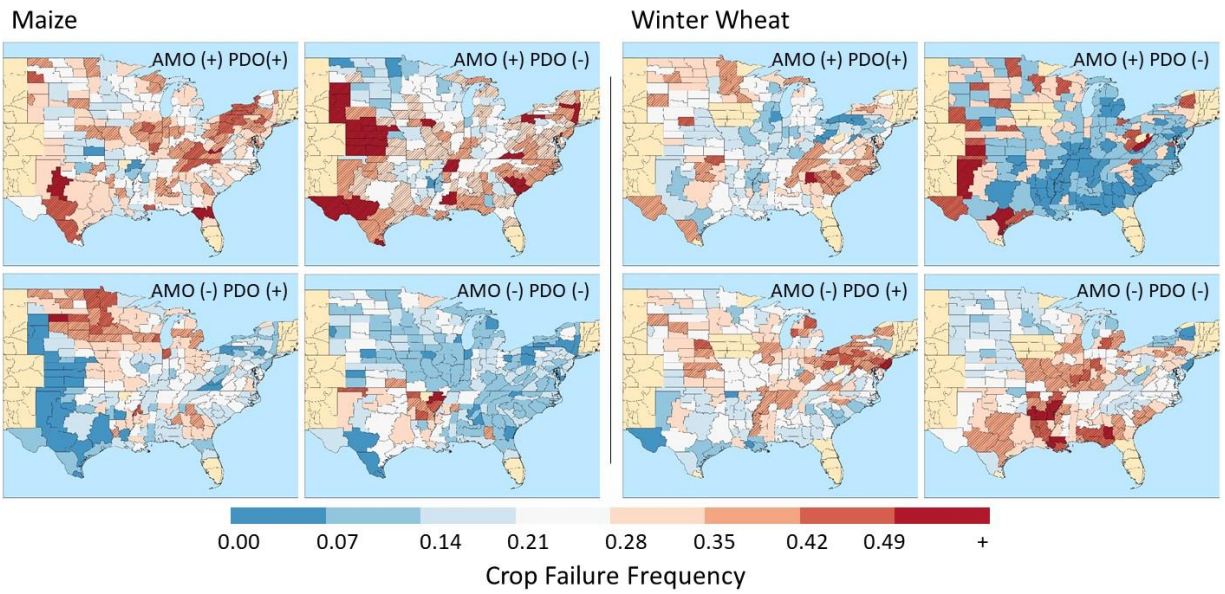


Figure 2.3 Annual crop failure frequency of maize during phase combinations of AMO and PDO for maize (four left images) and winter wheat (right four images). Climate divisions with blue coloring indicate a decrease in crop failure relative to the posterior distribution, while red divisions indicate an increase. Hashed climate divisions indicate significant increase in crop failure frequency at the 90th percentile.

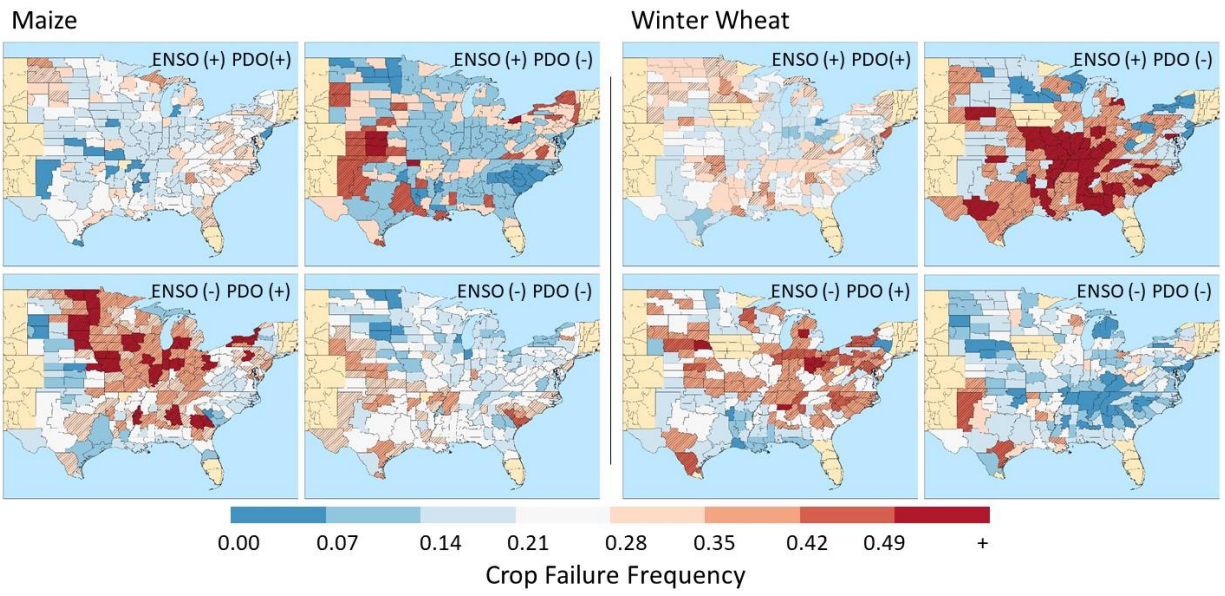


Figure 2.4 Same as in Figure 3 but for ENSO and PDO phase combinations.

Recommendations for future research

The findings of Chapters 1 and 2 contribute to the understanding of climate oscillations effects on maize and winter wheat in the United States. Chapter 2 stresses the importance to improve sub-seasonal to seasonal forecast for agricultural purposes.

This research focused on two major crops, one a summer crop (maize) and the other a winter crop (winter wheat). More crops can be included in future research including other cereal grains, legumes such as soybeans and peanuts, and cotton. Future research, especially regarding crop failure should be examined in conjunction with USDA Risk Management Agency (RMA) crop loss data sets. The addition of RMA data could potentially capture insurance claims of total crop loss resulting in no reported NASS yields, while also providing information about the type of loss validating suspected causes.

Five climate oscillations, AMO, NAO, ENSO, PDO, and PNA, were analyzed. These oscillations can be analyzed in more detail by conducting case studies on years of extreme yield and years when oscillation magnitude is high. Future research can potentially include other oscillations that may affect the United States.

This study area was largely rainfed with excellent data (yield, climate etc.) at sub-state levels. Providing an excellent foundation for oscillation impacts research. However, other breadbaskets exist elsewhere that could result in for security and global turmoil if yields are reduced. Therefore research can be expanded to include those and other regions to assess their vulnerability and improve seasonal forecasts.

References

- Akresh, R., Verwimp, P., & Bundervoet, T. (2011). Civil War, Crop Failure, and Child Stunting in Rwanda. *Economic Development and Cultural Change*, 59(4), 777–810. <https://doi.org/10.1086/660003>
- Allen, J. T., Tippett, M. K., & Sobel, A. H. (2015). Influence of the El Niño/Southern Oscillation on tornado and hail frequency in the United States. *Nature Geoscience*, 8(4), 278–283. <https://doi.org/10.1038/ngeo2385>
- Anderson, W., Seager, R., Baethgen, W., & Cane, M. (2018). Trans-Pacific ENSO teleconnections pose a correlated risk to agriculture. *Agricultural and Forest Meteorology*, 262(July), 298–309. <https://doi.org/10.1016/j.agrformet.2018.07.023>
- Asong, Z. E., Wheeler, H. S., Bonsal, B., Razavi, S., & Kurkute, S. (2018). Historical drought patterns over Canada and their teleconnections with large-scale climate signals. *Hydrology and Earth System Sciences*, 22(6), 3105–3124. <https://doi.org/10.5194/hess-22-3105-2018>
- Baum, M. E., Archontoulis, S. V., & Licht, M. A. (2019). Planting Date, Hybrid Maturity, and Weather Effects on Maize Yield and Crop Stage. *Agronomy Journal*, 111(1), 303. <https://doi.org/10.2134/agronj2018.04.0297>
- Benjamin, J. R., & Cornell, C. A. (1970). *Probability, Statistics, and Decisions for Civil Engineers*. New York: McGraw-Hill.
- Berglund, D. R., Endres, G. J., & McWilliams, D. A. (2013). Corn: Growth and Management Quick Guide. *Agronomist – Cereal Crops NDSU Extension Service*, 2(May), 1–8.
- Bollero, G. A., Bullock, D. G., & Hollinger, S. E. (1996). Soil Temperature and Planting Date Effects on Corn Yield, Leaf Area, and Plant Development. *Agronomy Journal*, 88(3), 385. <https://doi.org/10.2134/agronj1996.00021962008800030005x>
- Booth, B. B. B., Dunstone, N. J., Halloran, P. R., Andrews, T., & Bellouin, N. (2012). Aerosols implicated as a prime driver of twentieth-century North Atlantic climate variability. *Nature*, 484(7393), 228–232. <https://doi.org/10.1038/nature10946>
- Breiman, L. (2001). Random forests. *Machine Learning*, 45(1), 5–32. <https://doi.org/10.1023/A:1010933404324>
- Bureau of Labor Statistics, & U.S. Department of Labor. (1998). Three factors led to 1996 grain price shock. Retrieved June 19, 2019, from <https://www.bls.gov/opub/ted/1998/nov/wk1/art01.htm>
- Çakir, R. (2004). Effect of water stress at different development stages on vegetative and

- reproductive growth of corn. *Field Crops Research*, 89(1), 1–16.
<https://doi.org/10.1016/j.fcr.2004.01.005>
- Casella, G., & Berger, R. (2002). *Statistical Inference (Second Edition)* (2nd ed.). Pacific Grove, CA: Duxbury.
- Ceglar, A., Turco, M., Toreti, A., & Doblaz-Reyes, F. J. (2017). Linking crop yield anomalies to large-scale atmospheric circulation in Europe. *Agricultural and Forest Meteorology*, 240–241, 35–45. <https://doi.org/10.1016/j.agrformet.2017.03.019>
- Chahal, P. S., Aulakh, J. S., Jugulam, M., & Jhala, A. J. (2015). Herbicide-Resistant Palmer amaranth (*Amaranthus palmeri* S. Wats.) in the United States — Mechanisms of Resistance, Impact, and Management. In A. Price, J. Kelton, & L. Sarunaite (Eds.), *Herbicides, Agronomic Crops and Weed Biology*. InTech. <https://doi.org/10.5772/61512>
- Clement, A., Bellomo, K., Murphy, L. N., Cane, M. A., Mauritsen, T., Rädel, G., & Stevens, B. (2015). The Atlantic Multidecadal Oscillation without a role for ocean circulation. *Science (New York, N.Y.)*, 350(6258), 320–324. <https://doi.org/10.1126/science.aab3980>
- Climate Prediction Center Internet Team. (2012). Climate Prediction Center - Pacific/North American (PNA). Retrieved October 19, 2017, from <http://www.cpc.noaa.gov/data/teledoc/pna.shtml>
- Cole, J. E., & Cook, R. (1998). The Changing relationship between ENSO variability and moisture balance in the continental United States. *Geophysical Research Letters*, 25(24), 4529–4532.
- Coleman, J. S. M., & Budikova, D. (2013). Eastern U.S. summer streamflow during extreme phases of the North Atlantic oscillation. *Journal of Geophysical Research Atmospheres*, 118(10), 4181–4193. <https://doi.org/10.1002/jgrd.50326>
- Cook, R. J. (2001). Management of wheat and barley root diseases in modern farming systems. *Australasian Plant Pathology*, 30, 5–8. <https://doi.org/10.1071/AP01010>
- Cunfer, B. M. (2000). Stagonospora and Septoria diseases of barley, oat, and rye. *Canadian Journal of Plant Pathology*, 22(4), 332–348. <https://doi.org/10.1080/07060660009500452>
- Dahlman, L. (2009). Climate Variability: North Atlantic Oscillation | NOAA Climate.gov. Retrieved September 25, 2017, from <https://www.climate.gov/news-features/understanding-climate/climate-variability-north-atlantic-oscillation>
- Daly, C., Halbleib, M., Smith, J. I., Gibson, W. P., Doggett, M. K., Taylor, G. H., ... Pasteris, P. P. (2008). Physiographically sensitive mapping of climatological temperature and precipitation across the conterminous United States. *INTERNATIONAL JOURNAL OF CLIMATOLOGY Int. J. Climatol.* <https://doi.org/10.1002/joc.1688>
- Delworth, T., & Mann, M. E. (2000). Observed and simulated multi decadal variability in the Northern Hemisphere. *Clim. Dyn.*, 16, 661–676. <https://doi.org/10.1007/s003820000075>
- Denmead, O. T., & Shaw, R. H. (1960). The Effects of Soil Moisture Stress at Different Stages of Growth on the Development and Yield of Corn1. *Agronomy Journal*, 52(5), 272. <https://doi.org/10.2134/agronj1960.00021962005200050010x>

- Deser, C., Trenberth, K. E., & (Eds), N. C. for A. R. S. (2016). The Climate Data Guide: Pacific Decadal Oscillation (PDO): Definition and Indices.
- Deutsch, C. A., Tewksbury, J. J., Tigchelaar, M., Battisti, D. S., Merrill, S. C., Huey, R. B., & Naylor, R. L. (2018). Increase in crop losses to insect pests in a warming climate. *Science (New York, N.Y.)*, *361*(6405), 916–919. <https://doi.org/10.1126/science.aat3466>
- Di Liberto, T. (2016). Going out for ice cream: a first date with the Pacific Decadal Oscillation | NOAA Climate.gov. Retrieved October 18, 2017, from <https://www.climate.gov/news-features/blogs/enso/going-out-ice-cream-first-date-pacific-decadal-oscillation>
- Dima, M., & Lohmann, G. (2007). A hemispheric mechanism for the Atlantic multidecadal oscillation. *Journal of Climate*, *20*(11), 2706–2719. <https://doi.org/10.1175/JCLI4174.1>
- Durkee, J. D., Frye, J. D., Fuhrmann, C. M., Lacke, M. C., Jeong, H. G., & Mote, T. L. (2008). Effects of the North Atlantic Oscillation on precipitation-type frequency and distribution in the eastern United States. *Theoretical and Applied Climatology*, *94*(1–2), 51–65. <https://doi.org/10.1007/s00704-007-0345-x>
- Enfield, D. B., Mestas-Nuñez, A. M., & Trimble, P. J. (2001). The Atlantic multidecadal oscillation and its relation to rainfall and river flows in the continental U.S. *Geophysical Research Letters*, *28*(10), 2077–2080. <https://doi.org/10.1029/2000GL012745>
- FAO, IFAD, UNICEF, WFP, & WHO. (2018). *The State of Food Security and Nutrition in the World 2018. Building climate resilience for food security and nutrition*. Rome: Food and Agriculture Organization of the United Nations. Retrieved from www.fao.org/publications
- Foley, J. A., DeFries, R., Asner, G. P., Barford, C., Bonan, G., Carpenter, S. R., ... Snyder, P. K. (2005). Global Consequences of Land Use. *Science*, *309*(5734), 570–574. <https://doi.org/10.1126/science.1111772>
- Folland, C. K., Palmer, T. N., & Parker, D. E. (1986). Sahel rainfall and worldwide sea temperatures, 1901–85. *Nature*, *320*, 602–607. Retrieved from <https://www.nature.com/articles/320602a0.pdf>
- Fritsch, J. M., Kane, R. J., Chelius, C. R., Fritsch, J. M., Kane, R. J., & Chelius, C. R. (1986). The Contribution of Mesoscale Convective Weather Systems to the Warm-Season Precipitation in the United States. *Journal of Climate and Applied Meteorology*, *25*(10), 1333–1345. [https://doi.org/10.1175/1520-0450\(1986\)025<1333:TCOMCW>2.0.CO;2](https://doi.org/10.1175/1520-0450(1986)025<1333:TCOMCW>2.0.CO;2)
- Gaupp, F., Pflug, G., Hochrainer-Stigler, S., Hall, J., & Dadson, S. (2017). Dependency of Crop Production between Global Breadbaskets: A Copula Approach for the Assessment of Global and Regional Risk Pools. *Risk Analysis*, *37*(11), 2212–2228. <https://doi.org/10.1111/risa.12761>
- Gbegbelegbe, S., Chung, U., Shiferaw, B., Msangi, S., & Tesfaye, K. (2014). Quantifying the impact of weather extremes on global food security: A spatial bio-economic approach. *Weather and Climate Extremes*, *4*, 96–108. <https://doi.org/10.1016/J.WACE.2014.05.005>
- Gimeno, L., Ribera, P., Iglesias, R., de la Torre, L., García, R., & Hernández, E. (2002). Identification of empirical relationships between indices of ENSO and NAO and agricultural yields in Spain. *Climate Research*, *21*(2), 165–172.

<https://doi.org/10.3354/cr021165>

- Goodwin, B. K. (2001). Problems with Market Insurance in Agriculture. *American Journal of Agricultural Economics*, 83(3), 643–649. <https://doi.org/10.2307/1245093>
- Hall, R. G., & Nleya, T. (2012). iGrow Wheat : Best Management Practices for Wheat Production. In and K. D. lay, C. G. Carlson (Ed.). South Dakota State University.
- Hansen, J. W., Hodges, A. W., & Jones, J. W. (1998). ENSO influences on agriculture in the southeastern United States. *Journal of Climate*, 11(3), 404–411. [https://doi.org/10.1175/1520-0442\(1998\)011<0404:EIOAIT>2.0.CO;2](https://doi.org/10.1175/1520-0442(1998)011<0404:EIOAIT>2.0.CO;2)
- Hanway, J. J. (1963). Growth stages of corn (*Zea mays*, L.). *Agronomy Journal*, 55(5), 487–492. <https://doi.org/10.2134/agronj1963.00021962005500050024x>
- Heino, M., Puma, M. J., Ward, P. J., Gerten, D., Heck, V., Siebert, S., & Kummu, M. (2018). Two-thirds of global cropland area impacted by climate oscillations. *Nature Communications*, 9(1), 1–10. <https://doi.org/10.1038/s41467-017-02071-5>
- Henson, C., Market, P., Lupo, A., & Guinan, P. (2017). ENSO and PDO-related climate variability impacts on Midwestern United States crop yields. *International Journal of Biometeorology*, 61(5), 857–867. <https://doi.org/10.1007/s00484-016-1263-3>
- Hollinger, S. E., Isard, S. A., Hollinger, S. E., & Isard, S. A. (1994). A Soil Moisture Climatology of Illinois. *Journal of Climate*, 7(5), 822–833. [https://doi.org/10.1175/1520-0442\(1994\)007<0822:ASMCOI>2.0.CO;2](https://doi.org/10.1175/1520-0442(1994)007<0822:ASMCOI>2.0.CO;2)
- Hu, Z. Z., & Huang, B. (2009). Interferential impact of ENSO and PDO on dry and wet conditions in the U.S. great plains. *Journal of Climate*, 22(22), 6047–6065. <https://doi.org/10.1175/2009JCLI2798.1>
- Hurrell, J., & National Center for Atmospheric Research Staff, Ed. (2017). The Climate Data Guide. Hurrell North Atlantic Oscillation (NAO) Index (station-based). Retrieved from <https://climatedataguide.ucar.edu/climate-data/hurrell-north-atlantic-oscillation-nao-index-station-based>
- Hurrell, J. W. (1995). Decadal Trends in the North Atlantic Oscillation: Regional Temperatures and Precipitation. *Science*, 269(5224), 676–679. <https://doi.org/10.1126/SCIENCE.269.5224.676>
- Hurrell, J. W., Kushnir, Y., Ottersen, G., & Visbeck, M. (2003). *An overview of the North Atlantic Oscillation*. American Geophysical Union (AGU). <https://doi.org/10.1029/134GM01>
- Iizumi, T., Luo, J. J., Challinor, A. J., Sakurai, G., Yokozawa, M., Sakuma, H., ... Yamagata, T. (2014). Impacts of El Niño Southern Oscillation on the global yields of major crops. *Nature Communications*, 5(May), 1–7. <https://doi.org/10.1038/ncomms4712>
- Janetos, A., Justice, C., Jahn, M., Obersteiner, M., Glauber, J., & Mulhern, W. (2017). The Risks of Multiple Breadbasket Failures in the 21st Century: A Science Research Agenda, (March), 24. Retrieved from www.bu.edu/pardee

- Johnson, R. A., & Wichern, D. W. (2008). *Applied Multivariate Statistical Analysis, 6th Edition / Pearson* (6th ed.). Upper Saddle River, NJ: Pearson. Retrieved from <https://www.pearson.com/us/higher-education/program/Johnson-Applied-Multivariate-Statistical-Analysis-6th-Edition/PGM274834.html>
- Jones, J. W., Hansen, J. W., Royce, F. S., & Messina, C. D. (2000). Potential benefits of climate forecasting to agriculture. *Agriculture, Ecosystems & Environment*, 82(1–3), 169–184. [https://doi.org/10.1016/S0167-8809\(00\)00225-5](https://doi.org/10.1016/S0167-8809(00)00225-5)
- Kam, J., Sheffield, J., & Wood, E. F. (2014). Changes in drought risk over the contiguous United States (1901–2012): The influence of the Pacific and Atlantic Oceans. *Geophys. Res. Lett.*, 41, 5897–5903. <https://doi.org/10.1002/2014GL060973>. Received
- Kamara, A. Y., Menkir, A., Badu-Apraku, B., & Ibikunle, O. (2003). The influence of drought stress on growth, yield and yield components of selected maize genotypes. *The Journal of Agricultural Science*, 141(1), 43–50. <https://doi.org/10.1017/S0021859603003423>
- Karl, T. R., & Riebsame, W. E. (1984). The Identification of 10- to 20-Year Temperature and Precipitation Fluctuations in the Contiguous United States. *Journal of Applied Meteorology*. [https://doi.org/10.1175/1520-0450\(1984\)023<0950:TIOTYT>2.0.CO;2](https://doi.org/10.1175/1520-0450(1984)023<0950:TIOTYT>2.0.CO;2)
- Kellner, O., & Niyogi, D. (2015). Climate Variability and the U.S. Corn Belt: ENSO and AO Episode-Dependent Hydroclimatic Feedbacks to Corn Production at Regional and Local Scales*. *Earth Interactions D*, 19. <https://doi.org/10.1175/EI-D-14-0031.s1>
- Kerr, R. A. (2000). A North Atlantic Climate Pacemaker for the Centuries. *Science (New York, N.Y.)*, 288(5473), 1–10. <https://doi.org/10.1126/science.288.5473.1984>
- Kim, M. K., & McCarl, B. A. (2005). The agricultural value of information on the North Atlantic oscillation: Yield and economic effects. *Climatic Change*, 71(1–2), 117–139. <https://doi.org/10.1007/s10584-005-5928-x>
- Knight, J. R., Folland, C. K., & Scaife, A. A. (2006). Climate impacts of the Atlantic multidecadal oscillation. *Geophysical Research Letters*, 33(17), 2–5. <https://doi.org/10.1029/2006GL026242>
- Kogan, F. N. (2002). Droughts of the Late 1980s in the United States as Derived from NOAA Polar-Orbiting Satellite Data. *Bulletin of the American Meteorological Society*, 76(5), 655–668. [https://doi.org/10.1175/1520-0477\(1995\)076<0655:dotlit>2.0.co;2](https://doi.org/10.1175/1520-0477(1995)076<0655:dotlit>2.0.co;2)
- Kovats, R. S., Bouma, M. J., Hajat, S., Worrall, E., & Haines, A. (2003). El Niño and health. *The Lancet*, 362(9394), 1481–1489. [https://doi.org/10.1016/S0140-6736\(03\)14695-8](https://doi.org/10.1016/S0140-6736(03)14695-8)
- Lau, W. K. M., Kim, K.-M., Lau, W. K. M., & Kim, K.-M. (2012). The 2010 Pakistan Flood and Russian Heat Wave: Teleconnection of Hydrometeorological Extremes. *Journal of Hydrometeorology*, 13(1), 392–403. <https://doi.org/10.1175/JHM-D-11-016.1>
- Lauter, N., Kampani, A., Carlson, S., Goebel, M., & Moose, S. P. (2005). microRNA172 down-regulates glossy15 to promote vegetative phase change in maize. *Proceedings of the National Academy of Sciences of the United States of America*, 102(26), 9412–9417. Retrieved from www.pnas.org/cgi/doi/10.1073/pnas.0503927102

- Leathers, D. J., & Palecki, M. A. (1992). The Pacific/North American teleconnection pattern and United States climate. Part II: temporal characteristics and index specification. *Journal of Climate*. [https://doi.org/10.1175/1520-0442\(1992\)005<0707:TPATPA>2.0.CO;2](https://doi.org/10.1175/1520-0442(1992)005<0707:TPATPA>2.0.CO;2)
- Leathers, Daniel J., Yarnal, B., Palecki, M. A., Leathers, D. J., Yarnal, B., & Palecki, M. A. (1991). The Pacific/North American Teleconnection Pattern and United States Climate. Part I: Regional Temperature and Precipitation Associations. *Journal of Climate*. [https://doi.org/10.1175/1520-0442\(1991\)004<0517:TPATPA>2.0.CO;2](https://doi.org/10.1175/1520-0442(1991)004<0517:TPATPA>2.0.CO;2)
- Lesk, C., Rowhani, P., & Ramankutty, N. (2016). Influence of extreme weather disasters on global crop production. *Nature*, *529*(7584), 84–87. <https://doi.org/10.1038/nature16467>
- Li, S., & Bates, G. T. (2007). Influence of the Atlantic Multidecadal Oscillation on the winter climate of East China. *Advances in Atmospheric Sciences*, *24*(1), 126–135. <https://doi.org/10.1007/s00376-007-0126-6>
- Liaw, a, & Wiener, M. (2002). Classification and Regression by randomForest. *R News*, *2*(December), 18–22. <https://doi.org/10.1177/154405910408300516>
- Livezey, R. E., & Chen, W. Y. (1983). Statistical Field Significance and its Determination by Monte Carlo Techniques. *Monthly Weather Review*, *111*(1), 46–59. [https://doi.org/10.1175/1520-0493\(1983\)111<0046:SFSaid>2.0.CO;2](https://doi.org/10.1175/1520-0493(1983)111<0046:SFSaid>2.0.CO;2)
- Lott, N. (1993). *The summer of 1993 : flooding in the Midwest and drought in the Southeast*. Retrieved from <https://repository.library.noaa.gov/view/noaa/13836>
- Luxmoore, R. J., Fischer, R. A., Stolzy, L. H., & N, I. (1973). Flooding and Soil Temperature Effects on Wheat During Grain Filling. *Agronomy Journal*, *65*(3), 5–8. <https://doi.org/10.2134/agronj1973.00021962006500030006x>
- Mallya, G., Zhao, L., Song, X. C., Niyogi, D., & Govindaraju, R. S. (2013). 2012 Midwest Drought in the United States. *Journal of Hydrologic Engineering*, *18*(7). [https://doi.org/10.1061/\(ASCE\)HE.1943-5584.0000786](https://doi.org/10.1061/(ASCE)HE.1943-5584.0000786)
- Mangani, R., Tesfamariam, E., Bellocchi, G., Hassen, A., Mangani, R., Tesfamariam, E. H., ... Hassen, A. (2018). Growth, Development, Leaf Gaseous Exchange, and Grain Yield Response of Maize Cultivars to Drought and Flooding Stress. *Sustainability*, *10*(10), 3492. <https://doi.org/10.3390/su10103492>
- Mantua, N. J., & Hare, S. R. (2002). The Pacific Decadal Oscillation. *Journal of Oceanography*, *58*(1), 35–44. <https://doi.org/10.1023/A:1015820616384>
- Mantua, N. J., Hare, S. R., Zhang, Y., Wallace, J. M., & Francis, R. C. (1997). A Pacific interdecadal climate oscillation with impacts on salmon production. *Bulletin of the American Meteorological Society*, *78*(6), 1069–1079. [https://doi.org/10.1175/1520-0477\(1997\)078<1069:APICOW>2.0.CO;2](https://doi.org/10.1175/1520-0477(1997)078<1069:APICOW>2.0.CO;2)
- Mariotti, A. (2007). How ENSO impacts precipitation in southwest central Asia. *Geophysical Research Letters*, *34*(16), 2–6. <https://doi.org/10.1029/2007GL030078>
- Martinez, C. J., Baigorria, G. A., & Jones, J. W. (2009). Use of climate indices to predict corn yields in southeast USA. *International Journal of Climatology*, *29*(11), 1680–1691.

<https://doi.org/10.1002/joc.1817>

- Maxwell, J. T., Knapp, P. A., & Ortegren, J. T. (2013). Influence of the Atlantic Multidecadal Oscillation on tupelo honey production from AD 1800 to 2010. *Agricultural and Forest Meteorology*, *174–175*, 129–134. <https://doi.org/10.1016/j.agrformet.2013.02.014>
- McCabe, G. J., Palecki, M. A., & Betancourt, J. L. (2004). Pacific and Atlantic Ocean influences on multidecadal drought frequency in the United States. *Proceedings of the National Academy of Sciences of the United States of America*, *101*(12), 4136–4141. <https://doi.org/10.1073/pnas.0306738101>
- McKinnon, K. A., Rhines, A., Tingley, M. P., & Huybers, P. (2016). Long-lead predictions of eastern United States hot days from Pacific sea surface temperatures. *Nature Geoscience*, *9*(5), 389–394. <https://doi.org/10.1038/ngeo2687>
- Mendelsohn, R. (2007). What causes crop failure? *Climatic Change*, *81*(1), 61–70. <https://doi.org/10.1007/s10584-005-9009-y>
- Merry, M. (1991, July 26). Less wheat, greater need. *EIR*, p. 23. Retrieved from <https://larouchepub.com/eiw/public/1991/eirv18n28-19910726/index.html>
- Mills, C. M., & Walsh, J. E. (2013). Seasonal Variation and Spatial Patterns of the Atmospheric Component of the Pacific Decadal Oscillation. *Journal of Climate*, *26*, 1575–1594. <https://doi.org/10.1175/JCLI-D-12-00264.1>
- Mourtzinis, S., Ortiz, B. V., & Damianidis, D. (2016). Climate Change and ENSO Effects on Southeastern US Climate Patterns and Maize Yield. *Scientific Reports*, *6*(1), 29777. <https://doi.org/10.1038/srep29777>
- NASS. (2014a). *2012 Census of Agriculture, Farm and Ranch Irrigation Survey (2013), Volume 3, Special Studies Part 1*. Retrieved from https://www.nass.usda.gov/Publications/AgCensus/2012/Online_Resources/Farm_and_Ranch_Irrigation_Survey/fris13.pdf
- NASS. (2014b). *United States Summary and State Data Volume 1 • Geographic Area Series • Part 51*. Retrieved from https://www.nass.usda.gov/Publications/AgCensus/2012/Full_Report/Volume_1,_Chapter_1_US/usv1.pdf
- Neal, E. G., Walter, M. T., & Coffeen, C. (2002). Linking the pacific decadal oscillation to seasonal stream discharge patterns in Southeast Alaska. *Journal of Hydrology*, *263*, 188–197.
- Nleya, T. (2012). iGrow Wheat : Best Management Practices for Wheat Production. In D. E. Clay, C. G. Carlson, & K. Dalsted (Eds.) (p. Retrieved 8/8/14 from www.iGrow.org). South Dakota State University.
- NOAA. (1988). *The Drought of 1988 and Beyond*. Washington, DC. Retrieved from https://repository.library.noaa.gov/view/noaa/10952/noaa_10952_DS1.pdf
- Oerke, E. C. (2006). Crop losses to pests. *Journal of Agricultural Science*, *144*(1), 31–43. <https://doi.org/10.1017/S0021859605005708>

- Olgun, M., Metin Kumlay, A., Cemal Adiguzel, M., & Caglar, A. (2008). The effect of waterlogging in wheat (*T. aestivum* L.). *Acta Agriculturae Scandinavica, Section B - Plant Soil Science*, 58(3), 193–198. <https://doi.org/10.1080/09064710701794024>
- Opie, J. (1992). The Drought of 1988, the Global Warming Experiment, and Its Challenge to Irrigation in the Old Dust Bowl Region on JSTOR. *Agricultural History*, 66(2), 279–306. Retrieved from https://www.jstor.org/stable/3743858?read-now=1&seq=3#page_scan_tab_contents
- Porter, J. H., Parry, M. L., & Carter, T. R. (1991). The potential effects of climatic change on agricultural insect pests. *Agricultural and Forest Meteorology*, 57(1–3), 221–240. [https://doi.org/10.1016/0168-1923\(91\)90088-8](https://doi.org/10.1016/0168-1923(91)90088-8)
- Porter, J. R., & Gawith, M. (1999). Temperatures and the growth and development of wheat a review. *European Journal of Agronomy*, 10, 23–36.
- Ray, D. K., Gerber, J. S., Macdonald, G. K., & West, P. C. (2015). Climate variation explains a third of global crop yield variability. *Nature Communications*, 6, 1–9. <https://doi.org/10.1038/ncomms6989>
- Rippey, B. R. (2015). The U.S. drought of 2012. *Weather and Climate Extremes*, 10, 57–64. <https://doi.org/10.1016/J.WACE.2015.10.004>
- Rogers, Jeffery C., & Rogers, J. C. (1984). The Association between the North Atlantic Oscillation and the Southern Oscillation in the Northern Hemisphere. *Monthly Weather Review*, 112(10), 1999–2015. [https://doi.org/10.1175/1520-0493\(1984\)112<1999:TABTNA>2.0.CO;2](https://doi.org/10.1175/1520-0493(1984)112<1999:TABTNA>2.0.CO;2)
- Rogers, Jeffrey C., & Coleman, J. S. M. (2003). Interactions between the Atlantic Multidecadal Oscillation, El Niño/La Niña, and the PNA in winter Mississippi Valley stream flow. *Geophysical Research Letters*, 30(10), n/a-n/a. <https://doi.org/10.1029/2003GL017216>
- Rogers, Jeffrey C., Rohli, R. V., Rogers, J. C., & Rohli, R. V. (1991). Florida Citrus Freezes and Polar Anticyclones in the Great Plains. *Journal of Climate*, 4(11), 1103–1113. [https://doi.org/10.1175/1520-0442\(1991\)004<1103:FCFAPA>2.0.CO;2](https://doi.org/10.1175/1520-0442(1991)004<1103:FCFAPA>2.0.CO;2)
- Rosenzweig, C., Tubiello, F. N., Goldberg, R., Mills, E., & Bloomfield, J. (2002). Increased crop damage in the US from excess precipitation under climate change. *Global Environmental Change*, 12(3), 197–202. [https://doi.org/10.1016/S0959-3780\(02\)00008-0](https://doi.org/10.1016/S0959-3780(02)00008-0)
- Sacks, W. J., Deryng, D., Foley, J. A., & Ramankutty, N. (2010). Crop planting dates: an analysis of global patterns. *Global Ecology and Biogeography*, 19(5), 607–620. <https://doi.org/10.1111/j.1466-8238.2010.00551.x>
- Saini, H. S., & Westgate, M. E. (1999). Reproductive Development in Grain Crops during Drought. *Advances in Agronomy*, 68(C), 59–96. [https://doi.org/10.1016/S0065-2113\(08\)60843-3](https://doi.org/10.1016/S0065-2113(08)60843-3)
- Sarachik, E. S., & Cane, M. A. (2010). *The El Niño–Southern Oscillation Phenomenon*. Cambridge: Cambridge University Press. <https://doi.org/10.1017/CBO9780511817496>
- Schillerberg, T. A., Tian, D., & Miao, R. (2019). Spatiotemporal patterns of maize and winter

- wheat yields in the United States: Predictability and impact from climate oscillations. *Agricultural and Forest Meteorology*, 275(May), 208–222.
<https://doi.org/10.1016/j.agrformet.2019.05.019>
- Song, H., Li, Y., Zhou, L., Xu, Z., & Zhou, G. (2018). Maize leaf functional responses to drought episode and rewatering. *Agricultural and Forest Meteorology*, 249, 57–70.
<https://doi.org/10.1016/J.AGRFORMET.2017.11.023>
- Song, X.-P., Hansen, M. C., Stehman, S. V., Potapov, P. V., Tyukavina, A., Vermote, E. F., & Townshend, J. R. (2018). Global land change from 1982 to 2016. *Nature*.
<https://doi.org/10.1038/s41586-018-0411-9>
- Sperling, L. (1999). The effects of the Rwandan war on crop production, seed security and varietal security: a comparison of two crops. *War and Crop Diversity*, (150), 71–91.
 Retrieved from
https://www.researchgate.net/profile/Louise_Sperling2/publication/259459954_War_and_Crop_Diversity/links/550c3a550cf2ac2905a36343/War-and-Crop-Diversity.pdf#page=29
- Straus, D. M., & Shukla, J. (2002). Does ENSO force the PNA? *Journal of Climate*, 15(17), 2340–2358. [https://doi.org/10.1175/1520-0442\(2002\)015<2340:DEFTP>2.0.CO;2](https://doi.org/10.1175/1520-0442(2002)015<2340:DEFTP>2.0.CO;2)
- Sutton, R. T., & Hodson, D. L. R. (2005). Atlantic Ocean Forcing of North American and European Summer Climate. *Science*, 309(5731), 115–118.
<https://doi.org/10.1126/science.1109496>
- Teixeira, E. I., Fischer, G., van Velthuisen, H., Walter, C., & Ewert, F. (2013). Global hot-spots of heat stress on agricultural crops due to climate change. *Agricultural and Forest Meteorology*, 170, 206–215. <https://doi.org/10.1016/j.agrformet.2011.09.002>
- Tian, D., Asseng, S., Martinez, C. J., Misra, V., Cammarano, D., & Ortiz, B. V. (2015). Does decadal climate variation influence wheat and maize production in the southeast USA? *Agricultural and Forest Meteorology*, 204, 1–9.
<https://doi.org/10.1016/J.AGRFORMET.2015.01.013>
- Tian, D., Xie, G., Tian, J., Tseng, K.-H., Shum, C. K., Lee, J., & Liang, S. (2017). Spatiotemporal variability and environmental factors of harmful algal blooms (HABs) over western Lake Erie. *PLOS ONE*, 12(6), e0179622.
<https://doi.org/10.1371/journal.pone.0179622>
- Tigchelaar, M., Battisti, D. S., Naylor, R. L., & Ray, D. K. (2018). Future warming increases probability of globally synchronized maize production shocks. *Proceedings of the National Academy of Sciences of the United States of America*, 115(26), 6644–6649.
<https://doi.org/10.1073/pnas.1718031115>
- Ting, M. F., & Wang, H. (1997). Summertime US precipitation variability and its relation to Pacific sea surface temperature. *Journal of Climate*, 10(8), 1853–1873.
[https://doi.org/10.1175/1520-0442\(1997\)010<1853:suspva>2.0.co;2](https://doi.org/10.1175/1520-0442(1997)010<1853:suspva>2.0.co;2)
- Trenberth, K. E., Branstator, G. W., & Arkin, P. A. (1988). Origins of the 1988 North American drought. *Science*, 242(4886), 1640–1645. <https://doi.org/10.1126/science.242.4886.1640>
- Trenberth, K. E., & Shea, D. J. (2006). Atlantic hurricanes and natural variability in 2005.

- Geophysical Research Letters*, 33(12), 1–4. <https://doi.org/10.1029/2006GL026894>
- Trnka, M., Rötter, R. P., Ruiz-Ramos, M., Kersebaum, K. C., Olesen, J. E., Žalud, Z., & Semenov, M. A. (2014). Adverse weather conditions for European wheat production will become more frequent with climate change. *Nature Climate Change*, 4(7), 637–643. <https://doi.org/10.1038/nclimate2242>
- Troyanskaya, O., Cantor, M., Sherlock, G., Brown, P., Hastie, T., Tibshirani, R., ... Altman, R. B. (2001). Missing value estimation methods for DNA microarrays. *Bioinformatics*, 17(6), 520–525. <https://doi.org/10.1093/bioinformatics/17.6.520>
- United Press International. (1991). Rain Pares Size of US Wheat Harvest - CSMonitor.com. Retrieved May 27, 2019, from <https://www.csmonitor.com/1991/0613/13062.html>
- Vincenti-Gonzalez, M. F., Tami, A., Lizarazo, E. F., & Grillet, M. E. (2018). ENSO-driven climate variability promotes periodic major outbreaks of dengue in Venezuela. *Scientific Reports*, 8(1), 5727. <https://doi.org/10.1038/s41598-018-24003-z>
- Visbeck, M. (2002). North Atlantic Oscillation. Retrieved August 16, 2018, from www.ldeo.columbia.edu/NAO
- Wallace, J. M., & Gutzler, D. S. (1981). Teleconnections in the Geopotential Height Field during the Northern Hemisphere Winter. *Monthly Weather Review*. [https://doi.org/10.1175/1520-0493\(1981\)109<0784:TITGHF>2.0.CO;2](https://doi.org/10.1175/1520-0493(1981)109<0784:TITGHF>2.0.CO;2)
- Wang, G., & You, L. (2004). Delayed impact of the North Atlantic Oscillation on biosphere productivity in Asia. *Geophysical Research Letters*, 31(12), 4–7. <https://doi.org/10.1029/2004GL019766>
- Wegren, S. K. (2011). Food Security and Russia's 2010 Drought. *Eurasian Geography and Economics*, 52(1), 140–156. <https://doi.org/10.2747/1539-7216.52.1.140>
- Wen, C., Kumar, A., & Xue, Y. (2014). Factors contributing to uncertainty in Pacific Decadal Oscillation index. *Geophysical Research Letters*, 41(22), 7980–7986. <https://doi.org/10.1002/2014GL061992>
- Wilhelm, E. P., Mullen, R. E., Keeling, P. L., & Singletary, G. W. (1999). Heat stress during grain filling in maize: Effects on kernel growth and metabolism. *Crop Science*, 39(6), 1733–1741. <https://doi.org/10.2135/cropsci1999.3961733x>
- Wilks, D. S. (2011). *Statistical methods in the atmospheric sciences*. Elsevier/Academic Press.
- Wilson, L. M., Whitt, S. R., Ibáñez, A. M., Rocheford, T. R., Goodman, M. M., & Buckler, E. S. (2004). Dissection of Maize Kernel Composition and Starch Production by Candidate Gene Association. *The Plant Cell*, 16(10), 2719–2733. <https://doi.org/10.1105/TPC.104.025700>
- Zampieri, M., Ceglar, A., Dentener, F., & Toreti, A. (2017). Wheat yield loss attributable to heat waves, drought and water excess at the global, national and subnational scales. *Environmental Research Letters*, 12(6), 064008. <https://doi.org/10.1088/1748-9326/aa723b>
- Zhang, C. (2005). Madden-Julian Oscillation. *Reviews of Geophysics*, 43(2), RG2003. <https://doi.org/10.1029/2004RG000158>